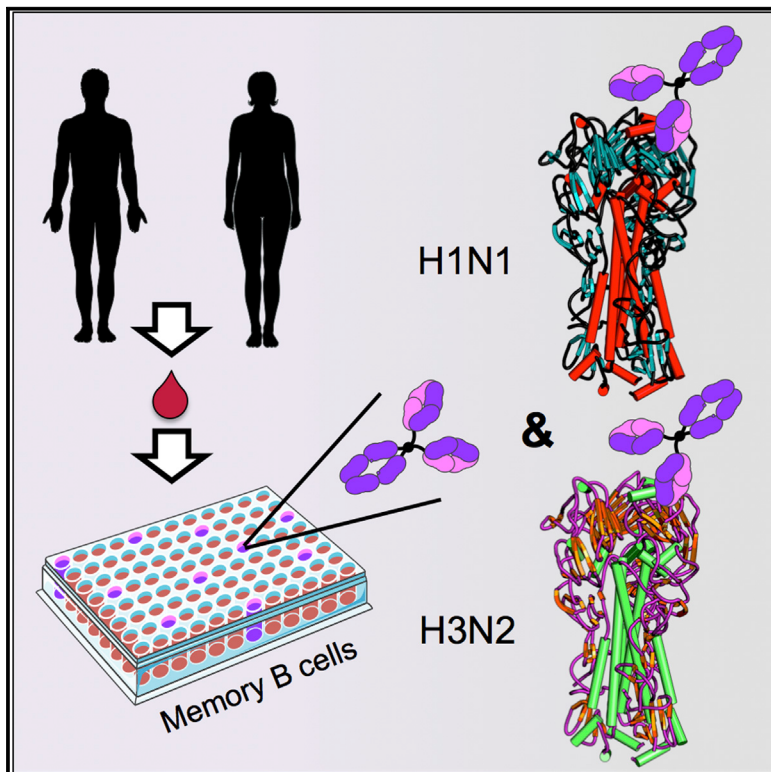


# Memory B Cells that Cross-React with Group 1 and Group 2 Influenza A Viruses Are Abundant in Adult Human Repertoires

## Graphical Abstract



## Highlights

- Human Bmem cells were found with BCRs cross-reactive for influenza A groups 1 and 2
- Cross-group Bmem cells were abundant, unlike cross-group serum antibodies
- Structures of HA receptor-site directed, cross-group antibodies showed key contacts
- Cross-group lineage antibodies were similar to a genetically unrelated antibody

## Authors

Kevin R. McCarthy, Akiko Watanabe,  
Masayuki Kuraoka, ...,  
Aaron G. Schmidt, Garnett Kelsoe,  
Stephen C. Harrison

## Correspondence

ghkelsoe@duke.edu (G.K.),  
harrison@crystal.harvard.edu (S.C.H.)

## In Brief

Hemagglutinins (HAs) from the two influenza A subtype groups have similar structures, but cross-reacting serum antibodies are rare. McCarthy et al. nonetheless found, in three donors, abundant cross-group B cell receptors (BCRs), many with epitopes on the HA head. Members of one clonal lineage had a BCR structure similar to that of a previously described, genetically unrelated antibody. Serial responses to seasonal influenza appear to have elicited the lineage and driven affinity maturation. Appropriate immunization regimens might elicit comparable responses.



# Memory B Cells that Cross-React with Group 1 and Group 2 Influenza A Viruses Are Abundant in Adult Human Repertoires

Kevin R. McCarthy,<sup>1,7</sup> Akiko Watanabe,<sup>3,7</sup> Masayuki Kuraoka,<sup>3</sup> Khoi T. Do,<sup>1</sup> Charles E. McGee,<sup>4</sup> Gregory D. Sempowski,<sup>4</sup> Thomas B. Kepler,<sup>5</sup> Aaron G. Schmidt,<sup>1,6</sup> Garnett Kelsoe,<sup>3,4,\*</sup> and Stephen C. Harrison<sup>1,2,\*</sup>

<sup>1</sup>Laboratory of Molecular Medicine, Boston Children's Hospital, Harvard Medical School, Boston, MA 02115, USA

<sup>2</sup>Howard Hughes Medical Institute, Boston, MA 02115, USA

<sup>3</sup>Department of Immunology, Duke University, Durham, North Carolina 27710, USA

<sup>4</sup>Duke Human Vaccine Institute, Duke University, Durham, North Carolina 27710, USA

<sup>5</sup>Department of Microbiology, Boston University School of Medicine, Boston, MA 02118, USA

<sup>6</sup>Present address: Ragon Institute of MGH, MIT and Harvard, Cambridge, MA 02139, USA, and Department of Microbiology and Immunobiology, Harvard Medical School, Boston, MA 02115, USA

<sup>7</sup>Contributed equally

\*Correspondence: ghkelsoe@duke.edu (G.K.), harrison@crystal.harvard.edu (S.C.H.)

<https://doi.org/10.1016/j.immuni.2017.12.009>

## SUMMARY

Human B cell antigen-receptor (BCR) repertoires reflect repeated exposures to evolving influenza viruses; new exposures update the previously generated B cell memory (Bmem) population. Despite structural similarity of hemagglutinins (HAs) from the two groups of influenza A viruses, cross-reacting antibodies (Abs) are uncommon. We analyzed Bmem compartments in three unrelated, adult donors and found frequent cross-group BCRs, both HA-head directed and non-head directed. Members of a clonal lineage from one donor had a BCR structure similar to that of a previously described Ab, encoded by different gene segments. Comparison showed that both Abs contacted the HA receptor-binding site through long heavy-chain third complementarity determining regions. Affinities of the clonal-lineage BCRs for historical influenza-virus HAs from both group 1 and group 2 viruses suggested that serial responses to seasonal influenza exposures had elicited the lineage and driven affinity maturation. We propose that appropriate immunization regimens might elicit a comparably broad response.

## INTRODUCTION

The natural history of human influenza viruses in the 20<sup>th</sup> and 21<sup>st</sup> centuries reflects the appearance of novel serotypes by transfer from avian or porcine reservoirs, alternating with periods of gradual antigenic change, during which each newly introduced virus evolves to reinfect previously immune individuals (Kilbourne, 2006; Smith et al., 2004). The immune repertoire of individual humans is largely the result of repeated exposures to evolving influenza viruses, beginning with infection (or recently, vaccination) early in life. The first exposure imprints the antigen-

receptor (BCR) repertoire of memory B cells (Bmem) and influences subsequent responses to influenza variants, owing to the combined effects of clonal selection during the primary response and subsequent recall and somatic evolution of cross-reactive Bmem cells following later infection or vaccination (Andrews et al., 2015; Fish et al., 1989; Fonville et al., 2014; Jensen et al., 1956; Lingwood et al., 2012; Pappas et al., 2014; Schmidt et al., 2015a). This history can be reconstructed from analysis of antibody clonal lineages (Lingwood et al., 2012; Pappas et al., 2014; Schmidt et al., 2015a). Rapid adaptation of the circulating influenza virus strain to resist prevalent immune responses results in a virus-antibody (Ab) evolutionary “arms race,” in which herd immunity selects for viral variants that escape neutralization and those variants in turn drive selection of somatically mutated B cells and Abs that overcome viral escape. We have shown in previous work that B cell clonal lineages from a single individual can illustrate the history of this arms race in the broader population (Raymond et al., 2016; Schmidt et al., 2015a).

The hemagglutinin (HA) of type A influenza virus, the more dominant of its two surface antigens, defines 18 serological subtypes, which fall into two evolutionarily distinguishable groups. Since 1977, viruses of two HA subtypes have co-circulated in human populations. The HAs of group 1 (of which the circulating H1 subtype is a member) and group 2 (e.g., the circulating H3 subtype) influenza viruses have very similar structures, but Abs that bind HAs from both groups are rare, even for epitopes that are functionally constrained and conserved, such as the receptor binding site (RBS) and the HA “stem” (Corti et al., 2011; Dreyfus et al., 2012; Kallewaard et al., 2016; Nakamura et al., 2013; Wrammert et al., 2011). Identification of BCRs that recognize HA epitopes shared by group 1 and group 2 influenza viruses in three adult subjects after immunization with trivalent influenza vaccine (TIV) has allowed us to characterize an instance of the evolutionary arms race between influenza viruses and the B cell responses of their hosts. We studied the Bmem BCR repertoires of these subjects using Nojima cultures (Kuraoka et al., 2016) to determine BCR specificity and avidity for single Bmem cells and to infer in each subject a history of clonal evolution in response to serial exposures to influenza variants.



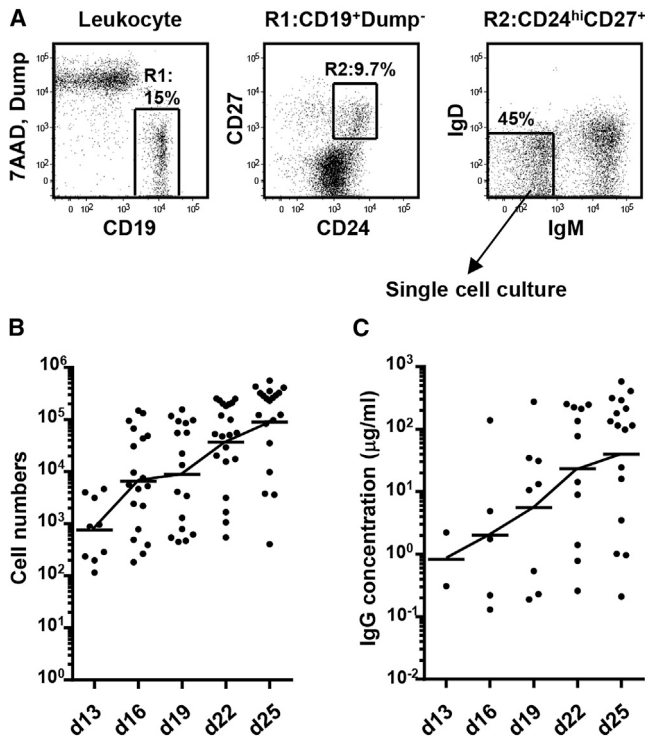


**Figure 1. Kinetics of B Cell Growth and IgG Concentrations in Single-Cell Cultures of Human Bmem Cells**

Single B cells were sorted from PBMCs and cultured in the presence of MS40L<sup>lo</sup> feeder cells with exogenous recombinant human IL-2, IL-4, IL-21, and BAFF. (A) Representative flow diagrams from 4 or more independent experiments showing the gating strategy used to isolate human Bmem cells (CD19<sup>+</sup>CD27<sup>+</sup>CD24<sup>hi</sup>IgM<sup>-</sup>IgD<sup>-</sup>).

(B and C) Kinetics of B cell numbers (B) and IgG concentrations in culture supernatants (C) during single-cell cultures of Ig class-switched Bmem cells. We analyzed 22 individual cultures from a single experiment for each time point; data shown are values for samples that exceeded the background for cell counting and IgG determinations.

This inferred history addresses questions relevant to understanding co-evolution of virus and host immune responses and to optimizing vaccination strategies. Are cross-reactive BCRs usually elicited by one serotype and “broadened” by subsequent exposure to another, related variant, and if so, does co-exposure to multiple serotypes offer any advantage? What are the differences among the epitopes on antigens from different strains that are recognized by cross-reactive Abs and what are the features of the antigen combining site (Ab paratope) that permit avid recognition of disparate influenza HAs? Are cross-reactive Bmem cells rare or common, and how closely does the Bmem BCR repertoire reflect that of serum IgG antibody? Answers to these questions are crucial for understanding how the humoral immune system generates and matures protective responses to influenza.

We show in the work reported here that a small but significant fraction ( $\approx 14\%$ ) of HA-specific Bmem cells from three unrelated, healthy donors expressed H3 and H1 cross-reactive BCRs. Most of these cross-reactive BCRs (42/55; 76%) were specific for the RBS or other epitopes present on the head of the HA trimer. We characterized in detail a substantial clonal

lineage (K03.1–12) comprising 12 members that avidly bind and neutralize both group 1 and 2 influenza viruses. The computationally inferred, unmutated common ancestor (UCA) of the lineage bound and neutralized H1 and H3 influenza viruses, demonstrating the capacity of germline BCRs to recognize the RBS of divergent influenza A subtypes. High resolution structural analysis of Ab-HA complexes showed that K03.1–12 lineage Abs contact the RBS through an extended HCDR3 loop. The interaction very closely resembled that of the RBS-directed paratope in a phage-display recombinant Ab, C05 (Ekiert et al., 2012). Although both AbC05 and the K03.1–12 lineage Abs bound the RBS identically, the V<sub>H</sub>, D<sub>H</sub>, and J<sub>H</sub> gene segments encoding these disparate Abs were not the same, suggesting that sequential exposure to seasonal HA variants might drive selection of common paratopic structures and that for some exposure sequences, such paratopes might afford protection against both H1 and H3 virus subtypes. Analysis of K03.1–12 lineage BCR affinities to historical HAs suggested that this lineage might have arisen in response to serial seasonal exposures to both HA serotypes, with a key event being the loss of the K133a residue in H1 HAs that occurred in 1995. These results suggest that appropriate immunization regimens could elicit comparably broad protection against infection by influenza A viruses.

## RESULTS

### Single-Cell Cultures of Human Bmem Cells Support Robust Proliferation and IgG Production

To obtain clonal IgG Abs from individual human Bmem cells, we adapted single-cell Nojima cultures (Kuraoka et al., 2016), as previously optimized for bulk expansions of human B cells (Su et al., 2016). We isolated CD19<sup>+</sup>CD27<sup>+</sup>CD24<sup>hi</sup>IgM<sup>-</sup>IgD<sup>-</sup> Bmem cells (Carsetti et al., 2004) from peripheral blood mononuclear cells (PBMCs) (Figure 1A) and cultured them on monolayers of MS40L-low feeder cells expressing human CD154 (Luo et al., 2009; Su et al., 2016). With the addition of human interleukin 2 (IL-2), IL-4, IL-21, and B cell activating factor (BAFF), this culture system supports B cell proliferation, Ig class-switch recombination, and differentiation into plasmablasts (Su et al., 2016) (Figure 1B). Thus, each culture supernatant contained a clonal IgG secreted by the differentiated progeny of individual Bmem cells (Figure 1C).

In culture, single Bmem cells multiplied to  $\approx 800$  cells by day 13 and then increased logarithmically to generate an average of 90,000 daughter cells by day 25 (Figure 1B). In some culture supernatants, we detected clonal IgGs as early as day 16; IgG concentrations rose to an average of 50  $\mu$ g/ml by day 25, with 56% of single B cell culture supernatants containing  $> 100 \mu$ g/ml IgG (Figure 1C). Cloning efficiency (IgG<sup>+</sup> cultures/total cultures) for human Bmem cells routinely exceeded 60%.

### Isolation of Individual rHA-Specific Human Bmem Cells

To characterize the BCR repertoire for recombinant influenza HA (rHA)-specific, IgG<sup>+</sup> Bmem cells, we sorted PBMCs from three unrelated, healthy donors who had received the 2014–15 TIV (KEL01 and KEL03) or the 2015–16 TIV (KEL06) two weeks before blood collection. We used PE-labeled rHA (H3N2 A/Wisconsin/67/2005, henceforth designated “H3 WI-05”) to enrich rHA-specific B cells, depositing one rHA<sup>+</sup>CD19<sup>+</sup>CD27<sup>+</sup>CD24<sup>hi</sup>IgM<sup>-</sup>IgD<sup>-</sup>IgG<sup>+</sup>

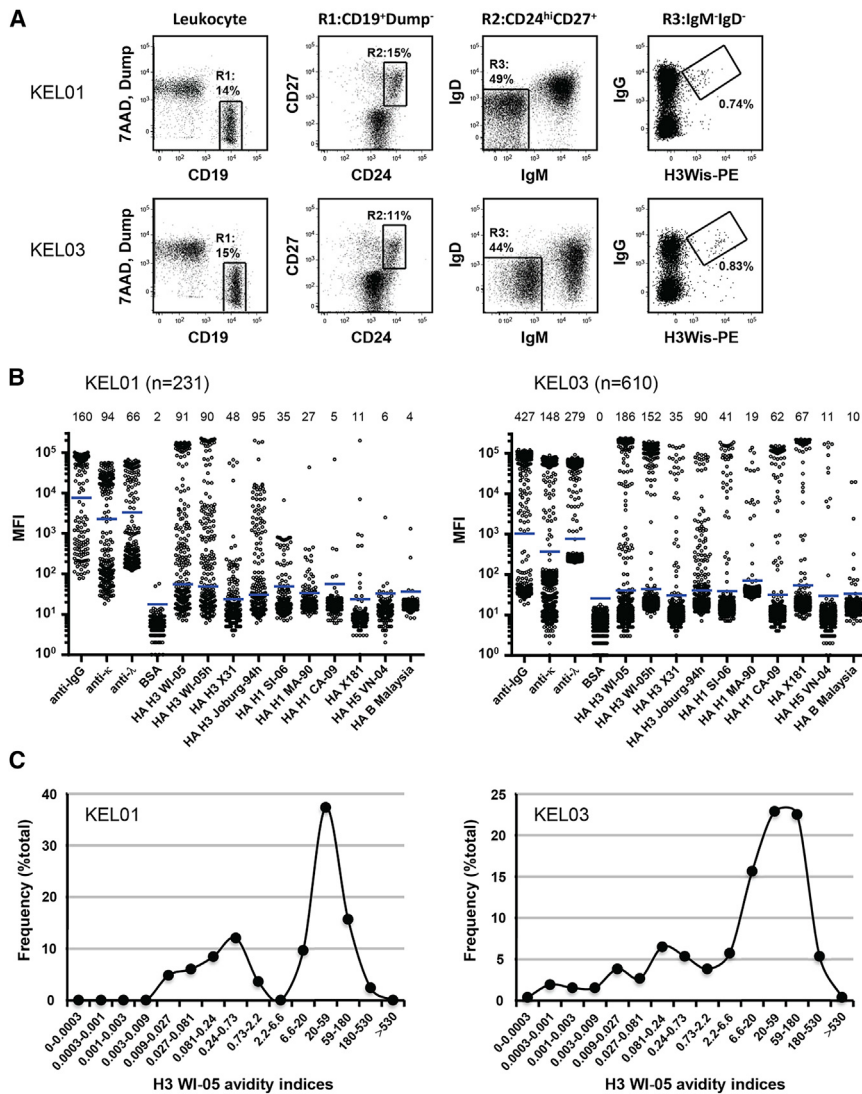


**Figure 2. Characterization of rHA-Specific Human Bmem Cells**

(A) Representative flow diagrams used to isolate rHA-specific IgG<sup>+</sup> human Bmem cells (H3 Wisconsin<sup>+</sup>CD19<sup>+</sup>CD27<sup>+</sup>CD24<sup>hi</sup>IgM<sup>+</sup>IgD<sup>-</sup>IgG<sup>+</sup>) from PBMCs of KEL01 and KEL03. Donors received TIV 2 weeks before blood collection.

(B) Representative Luminex diagram showing reactivity of culture supernatant IgGs from individual single B cell cultures (n = 231 for KEL01, n = 610 for KEL03) against 14 antigens including 4 positive and negative controls (anti-IgG, anti-IgM, anti-IgA, BSA) and a panel of rHAs (HA H3 WI-05 = H3 A/Wisconsin/67/2005; HA H3 X31 = H3 A/Aichi/2/1968 (X31); HA H1 SI-06 = H1 A/Solomon Islands/03/2006; HA H1 MA-90 = H1 A/Massachusetts/1/1990; HA H1 CA-09 = H1 A/California/04/2009; HA X181 = H1 A/reassortant/NYMC X-181 (California/07/2009 × NYMC X-157); HA H5 VN-04 = H5 A/Vietnam/1203/2004; and HA B Malaysia = B/Malaysia/2506/2004). We also included head-only HA constructs: HA H3 WI-05h = H3 A/Wisconsin/67/2005; and HA H3 Joburg-94h = H3 A/Johannesburg/33/1994. Each dot represents an individual test for each antigen. Bars in blue indicate the threshold median fluorescence intensities (MFIs) for each antigen (average + 6 SD of B cell negative, mock-treated samples). Above each column is the number of supernatants testing above this threshold.

(C) Distributions of rHA Avln for rHA (H3 WI-05)-reactive IgG<sup>+</sup> human Bmem cells relative to Ab2210 monoclonal standard. Curves were created by binning with 3-fold intervals Avln values for all samples. Data from one (for KEL01) and two individual experiments (for KEL03) are shown. See also Figures S1–S3 and Table S1.

memory cell per well (Figures 2A and S1A). Clonal IgGs that were later secreted into culture supernatants were individually screened against a panel of 10 rHA proteins in a multiplex bead assay (Figure 2B and Figure S1B).

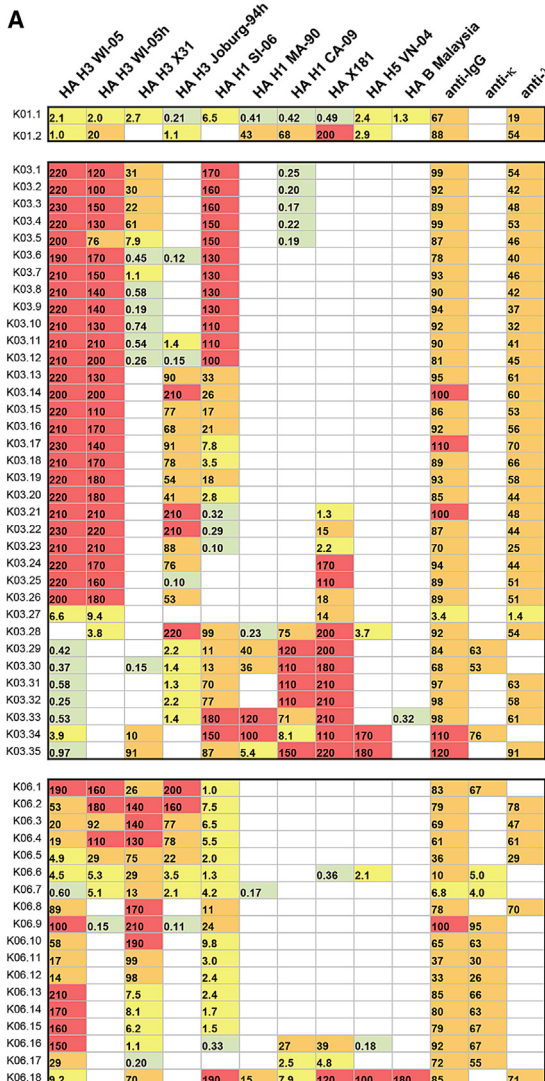
From a total of 874 IgG<sup>+</sup> wells (66% cloning efficiency), we identified 402 (46%) clonal IgGs with detectable affinity for the H3 Wi-05 rHA used in sorting. For both KEL01 and KEL03, avidity indices (Avlns; relative to the Ab2210 standard) for clonal IgGs (Kuraoka et al., 2016) clustered about a single, high-avidity peak that accounted for > 65% of the H3<sup>+</sup>IgG<sup>+</sup> cultures (Figure 2C). A lower avidity tail (Avln < 2.2) was also present (Figure 2C), as previously observed in mice immunized with an H1 rHA antigen (Kuraoka et al., 2016). For KEL06, avidity indices for clonal IgGs clustered about an intermediate-avidity peak, which accounted for > 65% of the H3<sup>+</sup>IgG<sup>+</sup> Bmem (Figure S1C). Despite these differences in the distributions of Avlns for H3<sup>+</sup>IgG<sup>+</sup> Bmem cells, serum titers against a panel of HAs were comparable for all three donors (Figure S2).

The screening panel included HAs from seasonal H3N2 viruses (in addition to H3 Wi-05), seasonal and new

pandemic H1N1 viruses, an H5N1 virus, and an influenza B virus (Figures 2B and 3A and S1B). Most KEL01 Bmem cells (89/91) were specific for H3 WI-05 and

other H3 subtypes, but two (2/91; 2%) avidly bound H3, H1, and H5 HAs, and one of these also bound B Malaysia HA (Figure 3A). Similarly, most Bmem clones from donor KEL03 were H3 specific (217/262), but 13% of them (35/262) also bound H1 (35/35) and H5 (3/35) HAs (Figure 3A); a third subset of Bmem clones (10/262) bound only weakly to H3 HAs but more avidly to HAs from non-H3 serotypes (Figure 2B). Over one-third of the H3<sup>+</sup>IgG<sup>+</sup> Bmem cells (18/49) from KEL06 also bound HAs from other subtypes: H1 (18/18), H5 (2/18), and B (1/18) (Figure 3A). All the crossreactive Bmem clones were HA specific and had little or no affinity for other protein antigens (Figure S3).

We further clustered crossreactive clonal IgGs by their patterns of reactivity with our panel of 10 rHAs (Figure 3A). The panel included two head-only constructs, which distinguish between antibodies that bind the HA head domains and those that bind elsewhere (“non-head”). Most of the crossreactive Bmem clones (35/37) from KEL01 and KEL03 reacted with the head of H3 WI-05 or H3 A/Johannesburg/3/1994 (H3 Jo’burg-94) or with both; the epitopes of crossreactive Bmem clones



from KEL06 were more evenly distributed between head (7/18) and non-head (11/18) (Figure 3A and Table S1). Of the head-directed, H3/H1 crossreactive clonal IgGs from the three donors, half (23/42), all from KEL03, inhibited binding of an RBS-specific monoclonal Ab, CH67 (Schmidt et al., 2013; Whittle et al., 2011), to the H1 A/Solomon Islands/3/2006 rHA (“H1 SI-06”) (Figure 3B) and hence bound epitopes proximal to the RBS. We conclude that a significant fraction (2%–37%) of HA-specific human Bmem clones recognized HAs from multiple influenza serotypes and that a substantial part of this cross-reactivity was for HA-head epitopes.

#### Broad BCR Diversity of H3 and H1 Cross-Reactive Human Bmem Cells

We amplified and sequenced heavy- and light-chain V(D)J rearrangements from the cross-reactive Bmem cell clones (Kuraoka et al., 2016; Tiller et al., 2008; Wardemann et al., 2003). No V(D)J rearrangement from a crossreactive Bmem cell was unmutated;  $V_H$  gene segments differed from their germline sequences by 4 to 38 point mutations, and  $V_L$  gene segments,

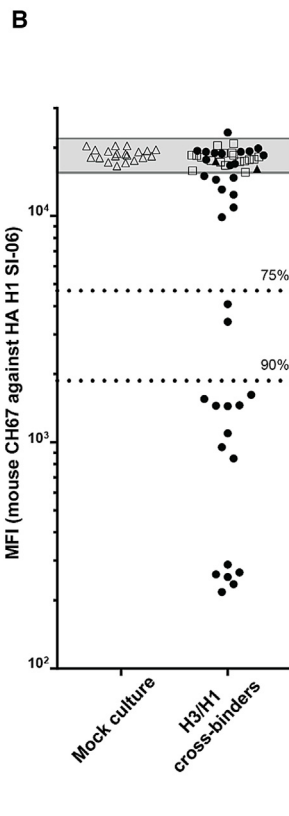


**Figure 3. Reactivity of H3 and H1 Cross-reactive Bmem Cells from Three Independent Donors**

Data for the 55 H3/H1 crossreactive Bmem cells from KEL01 ( $n = 2$ ), KEL03 ( $n = 35$ ) and KEL06 ( $n = 18$ ).

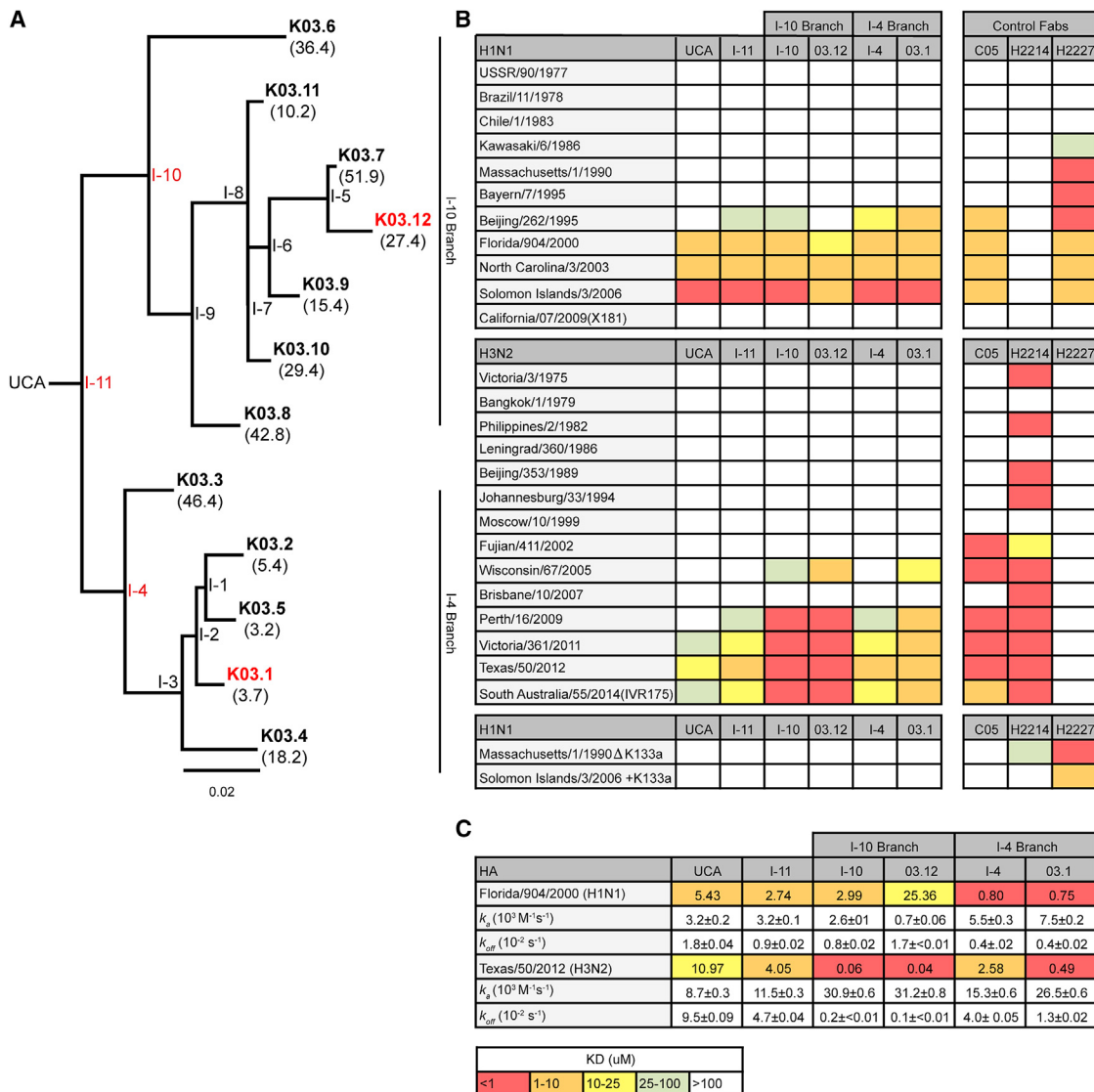
(A) MFI values from multiplex bead assay for indicated antigens, colored according to the key. (B) CH67 competition. All 55 clonal IgGs from the crossreactive Bmem cell cultures were tested for their capacity to inhibit binding to HA H1 SI-06 by RBS-directed monoclonal Ab, CH67. KEL01: closed triangles; KEL03: closed circles; KEL06: open squares. Culture supernatants from B cell negative wells (Mock culture;  $n = 20$ ) were used to establish threshold (mean  $\pm$  3SD, indicated as gray square). Dotted lines indicate MFI values corresponding to 75% and 90% inhibition, respectively. Each dot represents an individual sample. Representative data from two independent experiments are shown. See also Figure S4.

by 3 to 22 mutations (Figure S4). The two cross-reactive Bmem cells from donor KEL01 were clonally unrelated and used different  $V_H$  gene segments, IGHV3-23 and 4-61 (Figure S4). The H3 and H1 crossreactive Bmem cells from KEL03 ( $n = 35$ ) comprised five clonal lineages, containing between 2 and 12 members, and 7 singletons, and those from KEL06 ( $n = 18$ ), two clonal lineages, of 2 and 4 members, respectively, and 12 singletons (Figure S4). A total of 20 different V(D)J rearrangements were represented among the 28 distinct lineages and singletons from the three donors (Figure S4). The light-chain distribution was also broad (Figure S4). Thus, group 1 and group 2 crossreactive BCRs expressed by the cloned Bmem cells were genetically diverse, using different  $V_H$  and  $V_L$  gene segments to recognize epitopes shared by multiple HA subtypes.

#### Characterization of a Lineage of Cross-Group Binding Human Bmem Cells and Its UCA

The 12 member K03.1-12 lineage (Figure 4A) of H3/H1 crossreactive Bmem cells had distinctive features, including strong inhibition of CH67 binding and high avidity for both H3 WI-05 and H1 SI-06 HAs (Figure 3). We inferred the BCR of the lineage unmutated common ancestor (UCA), or presumptive founder, to have been encoded by rearrangements of IGHV1-2,IGHD6-19, and IGHJ6 and paired with IGLV2-23 joined to IGLJ2; the inferred UCA has an unusually long, 26-residue HCDR3 (Figure S4 and Supplemental Datasets 1 and 2).

We generated recombinant Abs (rAbs) representing key members of the K03.1-12 clonal lineage, including the UCA, for detailed characterizations of BCR specificity, affinity, and neutralization activity (Kuraoka et al., 2016). We screened Fabs of the K03.12 UCA, three inferred evolutionary intermediates

**Figure 4. Clonal Lineage K03.12 and Analysis of Affinity Maturation**

(A) Phylogram of K03.12 clonal antibody lineage, K03.1-12. Lineage members characterized further are in red. Avin for rHA (H3 WI-05) of each member in parentheses.

(B) Affinities of Fab fragments from selected lineage members for HA heads of seasonal H1 and H3 HAs that circulated during the donor's lifetime. Coloring according to the key indicates the apparent equilibrium dissociation constant ( $K_D$ ), measured by biolayer interferometry using a “single hit” Fab concentration of 30 μM. A second round of screening using UCA, K03.12 and K03.1 returned equivalent values.

(C) Affinity maturation of lineage K03.1-12.  $K_D$ s of lineage members for H1-FL-00 and H3 TX-12. See also Figure S5 and Table S2 and Supplemental Datasets 1 and 2.

(I-11, I-10, I-4), and two recovered members (K03.12 and K03.1) of the lineage for binding with a larger panel of HA heads from H1N1 and H3N2 viruses that circulated between the birth year (1975) of donor KEL03 and the year of sample collection (2014) (Figures 4B and S5). The UCA BCR bound strongly to the heads of HAs from H1N1 viruses that circulated between 2000 and 2006 and more weakly to the HA heads from H3N2 viruses that circulated between 2011 and 2014. Other lineage members bind the same HA heads, generally with higher affinity. Descendants of the UCA also bind heads of viral isolates that were not bound by the UCA (Figure 4B). Neutralization

assays gave similar results (Table S2). Neither the UCA nor K03.12 neutralized viruses that circulated before 2005. These data suggest that the UCA had the potential to bind both H3N2 and H1N1 HAs and that this property persisted during subsequent periods of affinity maturation.

#### Structures of K03.12 and the Lineage UCA, Bound with HA Head Domains

We determined the structure of the K03.12 Fab bound with the head domain of the HA from A/Texas/50/2012 (H3N2) (H3 TX-12), the H3 component of the 2014 vaccine given to the

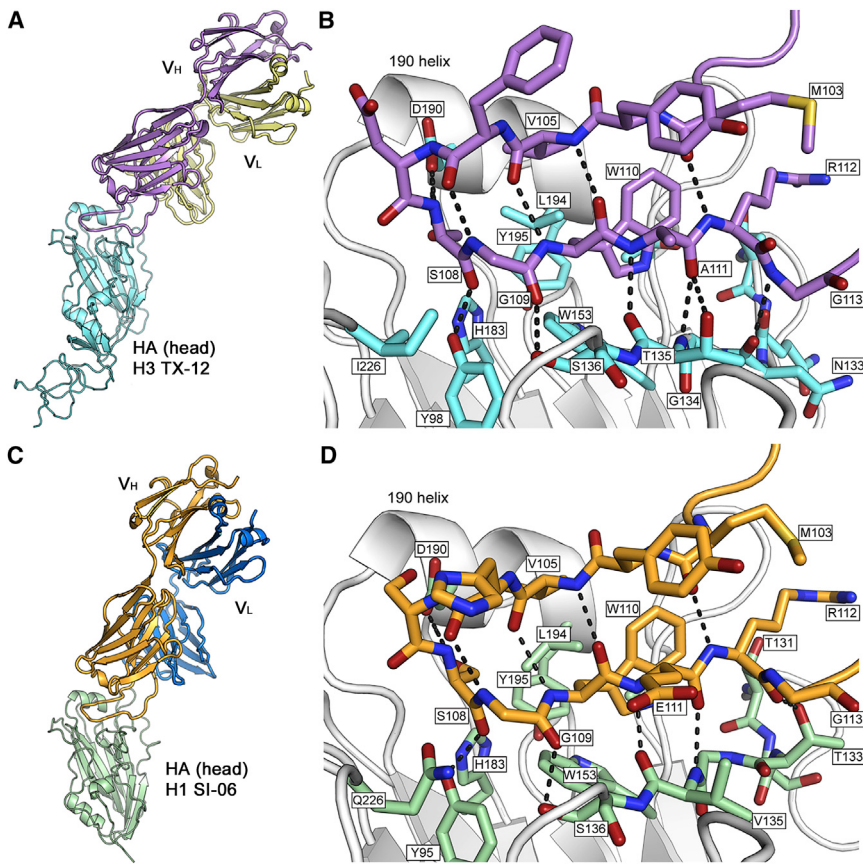


**Figure 5. Structures of K03.12 and UCA Bound with an HA Head**

(A) Structure of K03.12 bound with HA head of H3 TX-12.

(B) Contacts made by HCDR3 of K03.12 with conserved residues of the RBS; conserved HA residues, in cyan; K03.12 HCDR3, in purple.

(C) Structure of UCA bound with HA head of H1 SI-06. The SI-06 HA head is in the same orientation as the TX-12 head in Figure 4A.

(D) Contacts made by the UCA HCDR3 with conserved residues of the RBS. Conserved HA residues are in light green; the UCA HCDR3, in orange. See also Figure S6.

donor (Figure 5A). Contacts between Fab and HA were almost exclusively through the 26-residue HCDR3, the only exception being Glu 52 in LCDR2, which contacted Leu 157 (van der Waals contact) and Asn 158 (hydrogen bond) in HA. Ten residues of HCDR3 (103 to 112) formed an extended  $\beta$ -hairpin. Contacts with HA were principally with residues conserved (or conservatively substituted) in all H1 and H3 isolates—Tyr 98, Ser 136, Trp 153, Thr 155, Asp 190, and Leu 194 (Figure 5B). Moreover, main-chain hydrogen bonds with HCDR3 contributed a substantial component of the interaction, making binding less sensitive to the amino-acid sequence in HCDR3 than might otherwise be the case. For example, contacts that mimicked those from the carboxylate and acetamido groups of sialic acid (Schmidt et al., 2015b; Whittle et al., 2011) were with carbonyl 109 (with Ser 136) and the amide and carbonyl groups of residue 110 (augmenting the  $\beta$  hairpin of HCDR3 by an antiparallel  $\beta$ -interaction with HA residue 135).

We also determined the structure of the UCA Fab bound with the HA head domain from H1 SI-06 (Figure 5C). The contacts between the UCA HCDR3 and the H1 HA were essentially the same as those between K03.12 and the H3 HA (Figures 5D and S6), and the “footprints” of the two rAbs on HA were nearly identical.

The two structures show why members of the K03.1-12 lineage bound HAs of H1N1 viruses that circulated after about 1995 and why they failed to bind the new pandemic H1N1. The 1918 H1 HA, most of its descendants, and the 2009 new pandemic have, with respect to H3 HAs, an “extra” residue, conventionally numbered 133a, at the rim of the RBS. This residue displaces the strand

between residues 131 to 135 with respect to its conformation in H3 HAs and in H1 HAs that lack it; that displacement is incompatible with the observed positions of the HCDR3 in the two structures (Figure 6). Insertion of K133a into the H1 SI-06 HA eliminated binding of K03.1-12 lineage-member Fabs (Figure 4B). Deletion of K133a in some pre-1995 HAs was not, however, sufficient for high affinity of K03.12 or its UCA, nor were all post-1995 HAs that had lost the 133a residue high affinity antigens (Figure 4B).

A hinge at the base of the HCDR3  $\beta$ -hairpin, allowed K03.1-12 lineage antibodies to adapt to a relative shift of the H1 and H3 HA backbones at residue 133 without changing essential HCDR3 contacts. Although nearly all H1 HAs that circulated before 1995, as well as those of the 2009 pandemic and nearly all H5 HAs, have the 133a insertion, loss of residue 133a from H1 HAs did not lead to full coincidence of their polypeptide chain backbones with those of H3 HAs (Figure 6). Local sequence regularities cannot account for this consistent displacement, which appears to relate to a loop (residues 122–125) in HAs of group 1, absent in HAs of group 2, and with the identity of residue 152 (Asn in H1s; Leu in H3s). The 122–125 loop in H1 covers the hydrophobic Leu 152; absence of the loop favors a more polar residue, such as Asn 152, which in turn favors the “H3-like” configuration of the polypeptide-chain backbone at the 132–133 peptide bond by accepting a hydrogen bond from the position 133 main-chain amide (Figure 6). Indifference to these configurational variations will be a crucial property of any cross-reactive, RBS-directed antibody.

#### Analysis of Affinity Maturation in the K03.1-12 Lineage

The KEL03 donor was born in 1975, when the only circulating influenza A subtype was H3. H1 viruses re-emerged two years later, but not until 1995 would loss of residue 133a have allowed binding with K03.1-12 lineage members (<https://www.fludb.org/>). Thus, the lineage could have descended either from an early, subdominant, H3 response or from a post-1995, primary, H1 response. The lineage branched at intermediate I-11, which differed from the UCA at only two positions, one in HCDR3, the other at framework residue 18 in the light chain (Supplemental

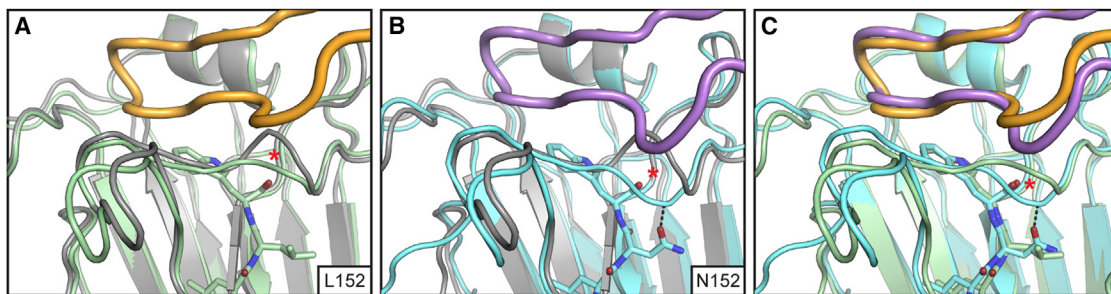


**Figure 6. Conformation of HA Residues 131-135**

(A) Polypeptide backbone of H1 CA-09 (PDB: 3UBE) (gray) superposed on HA backbone in the UCA-SI-06 complex (light green). Red asterisk: bulge spanning residues 131-135 (including 133a) in H1 CA-09.

(B) Polypeptide backbone of H1 CA-09 (PDB: 3UBE) (gray) superposed on HA backbone in the K03.12 - H3 TX-12 complex (purple and cyan, respectively). Red asterisk: close approach of K03.12 HCDR3 and bulge in H1 CA-09.

(C) Comparison of H1 (SI-06) and H3 (TX-12) backbones between residues 131 and 135. Red asterisk: polypeptide chain backbones of H1 (SI-06) and H3 TX-12 at position 133. Stick-representation of side-chain: residue 152, Leu or Ile in H1 HAs; Asn in H3 HAs. Dotted line: interaction in H3 HAs of the polypeptide chain backbone at position 133 with the side chain of Asn152.

**Dataset 2).** Neither mutation was at a position in contact with antigen. The HCDR3 mutation, a Tyr116Asp substitution, was present in all subsequent lineage members and created a salt bridge with Arg 112, which in turn donated a hydrogen bond to carbonyl 114 and another to Thr 131 in HA. The mutation could, in principle, have occurred during affinity maturation of the primary response. The interactions it introduced might have favored the H3-complementary configuration of the HCDR3 hinge.

The two branches of the K03.1-12 lineage had very different mutation frequencies—an average of about 7% in the I-10 branch and about half that in the I-4 branch while ratios of non-synonymous substitutions were similar in both branches (Figure S4). Differences in mutation density were already apparent in the intermediates, I-10 and I-4, that defined the two branches. Members of the I-10 branch bound H3 HAs more tightly than did members of the I-4 branch, a trend that could be seen in the H3-Wisconsin AvIn screen (Figures 3 and 4B). Conversely, members of the latter branch bound H1 HAs more avidly than did members of the former. Moreover, the affinity of K03.12 for H1 HAs was somewhat lower than that of its ancestors, I-10 and I-11. These comparisons suggest that H3 exposures might have driven affinity maturation and proliferation in the I-10 branch, and that H1 exposures might have driven the I-4 branch. At position 111, members of the I-4 branch retained a Glu residue in contact with the conserved Ser 145 in H1 HAs; the Glu111Ala mutation in the I-10 branch might reflect selection by the slightly larger Asn at the same position in most post-1975 H3 HAs. The re-introduction of K 133a in the new H1N1 pandemic of 2009, eliminating binding by any of these Abs, might account for the diminished affinity maturation in the H1-preferring I-4 branch and the continuing evolution in the H3-preferring I-10 branch.

#### Comparison of K03.12 with Ab C05

We found that the HA contacts of K03.12 were remarkably similar to those of a previously reported phage-library rAb, designated C05 (Ekert et al., 2012) (Figure 7). Although their heavy chains derived from completely different gene segments, both rAbs had HCDR3 loops of the same length and related amino acid

sequence. Their respective N-nucleotide sequences were very different, as expected for Abs that arose independently in different individuals (Figure S6). Nonetheless, sialic-acid-like contacts were essentially identical. Both Abs had a Trp at position 110 (100f in the C05 numbering), inserted in similar conformation into the hydrophobic slot between Trp 153 and Leu 194, where the acetamido methyl group of the sialic-acid receptor fits (Figure 7); both antibodies contacted HA residues 134–136 and Tyr 98 through homologous main-chain hydrogen bonds. C05 also shared with the UCA and the I-4 branch of the K03.1-12 lineage a Glu at position 111, which received a hydrogen bond from HA Ser145. The natural pairing of the C05 heavy chain is unknown, but the absence of substantial HA contacts from the light chain of either C05 or K03.12 probably allowed their heavy chains to be relatively promiscuous in light-chain association. The critical HA contacting residues (100c–100f) in the C05 HCDR3 were encoded primarily by N-nucleotides; the corresponding residues in the K03.1-12 lineage (107–110) were encoded by the human IGHD 6~19\*01 gene segment (Figure S7). Thus, both the human germline repertoire and junctional diversity can produce K03.1-12-like Abs with the capacity to neutralize group 1 and group 2 influenza viruses.

#### DISCUSSION

Nojima cultures, used here to analyze human responses to a TIV, are effective alternatives to single B cell sorting and V(D)J amplification and sequencing (Tiller et al., 2008; Wardemann et al., 2003). The efficacy of Nojima cultures is especially evident when seeking BCRs that are difficult to identify by flow cytometry because of their complex paratopic profiles (e.g., binding to several distinct antigens) or because they represent only a minor component of the B cell repertoire. The secretion of substantial quantities (> 50 µg/mL) of clonal IgG into Nojima culture supernatants of human Bmem cells permits rapid and repeated screening for BCR/IgGs with complex BCR binding profiles. Consequently, one can restrict V(D)J sequencing and recombinant IgG expression to just those BCRs of interest, having allowed the cloned B cells to do most of the work.

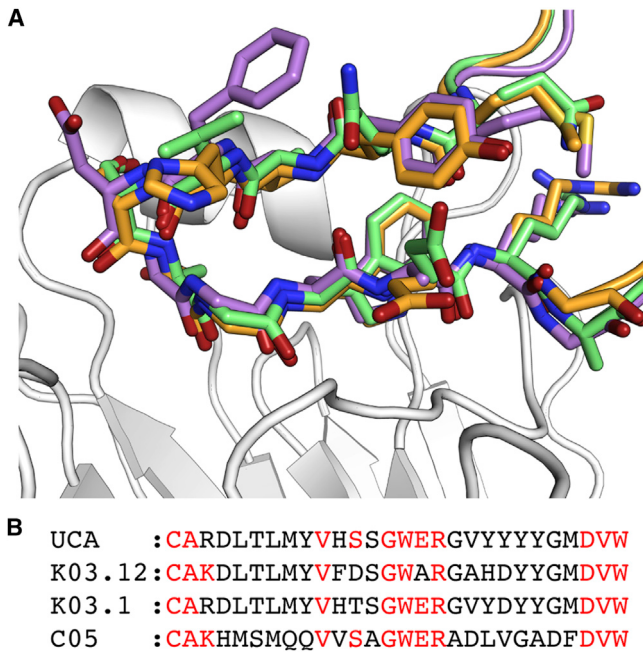


**Figure 7. Comparison of HCDR3 from K03.12 Lineage Members with that of Antibody C05**

(A) HA-Fab complexes of UCA, K03.12 and C05 (PDB: 4FP8) superposed on HA H3 TX-12. The HCDR3 of each Fab K03.12 (purple), UCA (orange), C05 (green) is shown in stick representation.

(B) Amino acid sequence alignment of HCDR3 in K03.12 lineage members and in antibody C05. Identical residues are in red. See also Figure S7.

Circulating influenza A viruses transmitted from one human to another recognize an  $\alpha$ -2,6 linked sialic acid receptor (Skehel and Wiley, 2000), and their receptor binding sites are correspondingly conserved, even across subtypes. Nonetheless, heterosubtypic, RBS-directed Abs have appeared only infrequently in published studies of the human B cell repertoire. The K03.1-12 lineage, inferred from the V(D)J sequences from 12 heavy and light-chain pairs recovered from single-cell Nojima cultures, offers a good opportunity to define specifically the antigenic ‘barriers’ that separate group 1 and group 2 HAs.

The presence of residue 133a adds a bulge to the backbone conformation on the lateral edge of the RBS, but there is a consistent difference at position 133 between H3 HAs and even those H1 and H5 HAs that lack residue 133a. The lineage of any RBS-directed antibody sensitive to this difference may fail to develop heterosubtypic breadth, even after repeated exposure to HAs of the heterologous group. The adaptability of Abs in the K03.1-12 lineage might come from configurational flexibility at Gly 113, which has a negative  $\phi$  torsion angle in the K03.12 complex with an H3 HA and a positive one in the UCA complex with an H1 HA, allowing the C-terminal side of HCDR3 to move away from residue 133 in the latter. C05 has an Ala at the position corresponding to 113, but the configuration of its polypeptide chain at the C-terminal end of HCDR3 suggests that the Fab could bind H1 HAs with only a small adjustment of the configuration seen in the published X31 (H3) complex (Ekert et al., 2012). Neither C05 nor members of the K03.1-12 lineage can bind HAs bearing residue 133a (e.g., the new pandemic A/California/07/2009).

Another characteristic difference between group 1 and group 2 HAs is the identity of residue 226 (Lin et al., 2012), which is also a key site of change when avian viruses adapt to human receptors (Rogers et al., 1983). The UCA HCDR3 avoids this residue in its complex with Gln 226 in H1 SI-06, and K03.12 itself has a single van der Waals contact with Ile 226 in H3 TX-12. Lineage members can also bind H1 HAs with Arg 226, an adaptation to growth in eggs found in some vaccine strains (Raymond et al., 2016).

The affinities of K03.1-12 lineage Fabs for HAs from virus isolates circulating during the donor’s lifetime suggest two alternative histories for their elicitation and affinity maturation. The earliest HA in our panel that binds the K03.1-12 lineage UCA Fab is an H1 from the year 2000. The structures show that the presence of residue 133a in H1 HAs is incompatible with binding by K03.1-12 lineage members and hence that if the eliciting exposure was to an H1 HA, the primary response was unlikely to have occurred before 1995—the antigenic cluster transition that accompanied 133a loss. The affinities for H1 HAs of K03.12, K03.1, and lineage intermediates increased between 2000 and 2006, but so did the affinity of the UCA, showing that the increases were due primarily to mutational changes in the HAs, not in the antibodies. For H3 isolates, however, the relative affinities of various lineage intermediates probably do reflect ongoing affinity maturation. Thus an alternative history of the lineage invokes a subdominant response to an H3 virus, perhaps during the donor’s childhood (e.g., 1975–1980). Loss of residue 133a from H1 HAs—and hence emergence of a more H3-like epitopic contact—could then have stimulated clonal expansion in the late 1990’s, followed by a further wave of affinity maturation against H3s after 2009. A suspected influenza infection around the year 2000, reported by donor KEL03, might have accounted for the former, H1-based diversification. Our earlier analysis of GC B cells in mice immunized with HA showed both a diversifying repertoire in primary GCs and retention of lower avidity clones (Kuraoka et al., 2016). Both observations suggested that the response to complex antigens might have evolved to retain a heterogeneity of avidities and a diversity of epitopic specificities, to optimize protection against subsequent exposures to antigenic variants of a pathogen.

The congruence of the C05 and K03.1-12 HCDR3 loops is a striking example of two essentially identical antigen combining sites in BCRs from unrelated donors. That we found this convergent evolution in a relatively small sample of Bmem cells suggests that the H3 and H1 cross-reactive BCR paratope is not particularly rare. Unlike VRC01-like Abs that react with the HIV-1 RBS (Zhou et al., 2010), the K03.1-12 paratope that interacts with the RBS of H1 and H3 HAs is not a germline-encoded element but part of an HCDR3 loop encoded, at 11 of its 26 amino-acid residues, by N-nucleotides. The 26-residue HCDR3 is about 10 residues longer than the mean length of human HCDR3s and therefore thought to be disfavored (Willis et al., 2016). An extensive study of long HCDR3 sequences in a cohort of adult, HIV-naïve donors found a frequency of about 1% for 26-residue HCDR3s, with a bias toward J<sub>H</sub>6 encoded J-segments (as in K03.12) and about a 4% representation of IGHD 6-19 encoded D-segments (with two possible open reading frames) (Willis et al., 2016). The probability of finding a K03.12-like antibody among the corresponding 0.02% of all BCRs in an

individual will thus depend on how restrictive are the requirements for particular amino-acid residues at particular N-nucleotide encoded positions in the loop. The high proportion of backbone (rather than side-chain) interactions with the HA RBS, suggest that potential germline precursors of K03.1-12-like Abs could be present in most human naive B cell repertoires. We searched for KEL03.12-like HCDR3 sequences among BCR sequences from a cohort that received the 2008 TIV (Jackson et al., 2014). The cells from five of the 14 subjects yielded least one sequence encoding a long HCDR3 similar to that of KEL03.12, and five of the seven KEL03.12-like sequences identified were from cells isolated at various intervals following vaccine administration.

In all three of the normal donor samples analyzed by Nojima cultures, we found a cross-reactive BCR phenotype with substantial representation (2%–37%) among H3-binding Bmem cell clones; most (76%) recognized HA head epitopes. The relative abundance in these individuals of human Bmem cells that cross-reacted with the HA head from group 1 and group 2 influenza contrasts with results of a recent study (Joyce et al., 2016) in which Bmem cells cross-reacting with HAs from group 1 and group 2 influenza A were found to be specific for stem epitopes. The differences in our observations may reflect different strategies for recovering Bmem populations. (1) The sorting criteria were different: selection of H5<sup>+</sup>H7<sup>+</sup> double-positive Bmem (Joyce et al., 2016) versus H3<sup>+</sup> single-positive Bmem (this work). The RBS of our H3 probe is not only very similar to the corresponding site on the H3s that imprinted and updated these individuals' repertoires, but it is also more similar to the H1 RBS in viruses circulating since 1995 than it is to those of H5 or H7 (or essentially any other avian strain). The affinity of an H1 or H3 imprinted repertoire for the RBSs of H5 and H7 might have been too low for robust detection in the sorting step. Moreover, stem-directed Bmem cells appear to be in low abundance in most individuals, probably because on the virions that would have elicited the imprinting response during a childhood infection, the stem is relatively inaccessible. Therefore, in an H3 sort, RBS-directed Bmem BCRs present at the time of vaccination would probably have dominated the crossreactive component of the Bmem cells detected. In an H5 plus H7 sort, however, the stem would be the only epitope similar enough to those on H1 or H3 HAs to yield a positive signal. (2) The fluorescent H3-HA that we used to isolate Bmem cells had a wild-type RBS instead of a modified “bait” with a mutation (Y98F), introduced to eliminate sialic-acid binding and hence prevent the staining of non-HA binding cells (Whittle et al., 2014). Y98 contacts KEL03.12 and other RBS directed antibodies. It is possible that this mutation might have prevented or diminished the labeling of HA-head reactive cells. (3) A further difference between the studies is analysis of only expanded clonal lineages (Joyce et al., 2016) versus analysis of all HA-binding clones (this work). The nearly equal representation of head- and non-head directed H3/H1 crossreactive Bmem cells from donor KEL06 shows that we could readily identify both. (4) Finally, there were distinct exposure histories by vaccination or infection of the disparate donors in each study.

Regardless of these methodological differences, our results show that the human immune system can provide protection against divergent influenza A virus types through common

epitopes that are present on the HA head, as well as through those on the stem. At least one of these common epitopes is the RBS.

The relative abundance of human Bmem cells expressing H3/H1 cross-reactive, head-directed BCRs contrasts with the infrequent detection of crossreacting serum antibodies reported in the literature (Corti et al., 2011; Dreyfus et al., 2012; Kallewaard et al., 2016; Nakamura et al., 2013; Wrammert et al., 2011). It is possible that distinct compartments of the humoral response—here, Bmem cells and the plasmacytes that produce serum antibody (Nutt et al., 2015)—do not generally reflect a common BCR repertoire. If so, analyses of serum antibody reactivity against influenza HAs might not report the full spectrum of BCR specificities in Bmem populations elicited by infection or vaccination. Indeed, serum IgG antibody for H3 WI-05 did not reflect differences in the distributions of Avlins for HA H3 WI-05 reactive Bmem cells recovered from the KEL01, –03, and –06 donors. High affinity BCRs promote differentiation of GC B cells into long-lived plasmacytes, while GC B cells with lower affinity receptors enter the Bmem compartments (Kräutler et al., 2017; Phan et al., 2006). This selection might be driven by intrinsic differences in BCR signaling or might reflect a “temporal switch” in the GC reaction that favors generation of long-lived plasmacytes late in the GC response (Weisel et al., 2016). These differences suggest that the Bmem pools sampled by Nojima culture might represent populations that are less avid but more crossreactive than BM plasmacytes.

The course of affinity maturation in the two branches of the K03.1-12 clonal lineage indicates that donor KEL03 experienced a succession of exposures to influenza A viruses (or vaccine HAs) of both subtypes. We note the HAs used to pan for C05 were similar to those used in this study: H3-Wisconsin and A/New Caledonia/20/1999 (H1N1), an H1N1 virus that also lacked the K133a insertion. In these examples, selection for binding to similar HAs resulted in a common solution. This result shows that a suitably chosen sequence of vaccine immunogens might favor a similar heterosubtypic response (Haynes et al., 2012).

## STAR★METHODS

Detailed methods are provided in the online version of this paper and include the following:

- KEY RESOURCES TABLE
- CONTACT FOR REAGENT AND RESOURCE SHARING
- EXPERIMENTAL MODEL AND SUBJECT DETAILS
  - Subject Details
  - Cell Lines
  - Subject-Derived Cells
- METHOD DETAILS
  - Clinical Samples
  - Flow Cytometry and Human Bmem Cell Definition
  - Single-Cell Cultures for Human Bmem Cells
  - BCR Rearrangement Amplification and Analysis
  - Multiplex Bead Assay
  - CH67 Inhibition Assay
  - Recombinant Fab Expression and Purification

- Recombinant IgG Expression and Purification
- Recombinant HA Expression and Purification
- Biolayer Interferometry (BLI)
- Virus Propagation
- Influenza Microneutralization Assay
- Crystallization
- Structure Determination and Refinement
- QUANTIFICATION AND STATISTICAL ANALYSIS
- Binding Studies
- Neutralization Assays
- DATA AND SOFTWARE AVAILABILITY

## SUPPLEMENTAL INFORMATION

Supplemental Information includes seven figures, three tables, and two data-sets and can be found with this article online at <https://doi.org/10.1016/j.immuni.2017.12.009>.

## ACKNOWLEDGMENTS

We thank Goran Bajic, Simon Jenni, Tim Caradonna, and Lindsey Robinson-McCarthy for advice, discussion, and instruction; Allan Parelli (BCH), Xiaoyan Nie and Xiao Liang (Duke Immunology), and Ariel K. Mason and Christopher Sample (Duke RBL) for technical assistance; Kevin Wiehe and Amy Wang for a preliminary clonal lineage analysis. Affinity measurements were carried out in the Harvard Medical School Center for Macromolecular Interactions, directed by Dr. Kelly Arnett. X-ray diffraction data were recorded at beamline 8.2.2 (operated by the Berkeley Center for Structural Biology and the Howard Hughes Medical Institute) at the Advanced Light Source (ALS, Lawrence Berkeley Laboratory) and at beamline ID-24-C (operated by the Northeast Collaborative Access team: NE-CAT) at the Advanced Photon Source (APS, Argonne National Laboratory). We thank the staff members at both beamlines for advice and assistance in data collection. Influenza stock propagation and microneutralization assays were performed in the Virology Unit of the Duke Regional Biocontainment Laboratory (RBL), managed by C.E.M. and directed by G.D.S. The Duke RBL received partial support for construction from the National Institutes of Health and National Institute of Allergy and Infectious Diseases (UC6-AI058607). The following reagents were obtained through BEI Resources, NIAID, NIH: Kilbourne F165: A/Chile/1/1983 (HA, NA) x A/Puerto Rico/8/1934 (H1N1), Reassortant X-83, NR-3585; Kilbourne F178: A/Shanghai/11/1987 (HA, NA) x A/Puerto Rico/8/1934 (H3N2), High Yield, Reassortant X-99a, NR-3505; Kilbourne F86: A/Johannesburg/33/1994 (HA, NA) x A/Puerto Rico/8/1934 (H3N2), Reassortant X-123a, NR-3580; Influenza A Virus, A/California/07/2009 (H1N1)pdm09 Egg Isolate (Produced in Eggs), NR-13663; and Ferret Hyperimmune Sera to Influenza A/California/07/2009 (H1N1)pdm09, NR-19261; and Monoclonal Anti-Influenza A Virus Nucleoprotein (NP), Clones A1 and A3 (ascites blend, Mouse), NR-4282. The following reagent was obtained through the NIH Biodefense and Emerging Infections Research Resources Repository, NIAID, NIH: Ferret Hyperimmune Sera to Influenza A/Solomon Islands/3/2006 (H1N1), NR-19262. Influenza A Virus, A/Wisconsin/67/2005 (H3N2), FR-397; Influenza A Virus, A/Solomon Islands/3/2006 (H1N1), FR-331; Influenza A Virus, A/Texas/50/2012 (H3N2), FR-1210; Ferret Antisera to Influenza A Virus, A/USSR/90/1977 (H1N1), FR-953; Ferret Antisera to Influenza A Virus, A/Fujian/411/2002 (H3N2), FR-1264; Ferret Antisera to Influenza A Virus, A/Texas/50/2012 (H3N2), FR-1263; and Madin-Darby Canine Kidney (MDCK) Cells, London Line, FR-58, was obtained through the Influenza Reagent Resource, Influenza Division, WHO Collaborating Center for Surveillance, Epidemiology and Control of Influenza, Centers for Disease Control and Prevention, Atlanta, GA, USA. NE-CAT is funded by NIH grant P41 GM103403 and the Pilatus 6M detector on 24-ID-C by NIH-ORIP HEI grant S10-RR029205. APS is operated for the DOE Office of Science by Argonne National Laboratory under contract DE-AC02-06CH11357. The research was supported by NIH grants P01 AI089618 (to S.C.H.), U19 AI117892 (to G.K. and T.B.K.), and R01 AI128832 (to G.K.). S.C.H. is an Investigator in the Howard Hughes Medical Institute.

## AUTHOR CONTRIBUTIONS

Designed experiments: K.R.M., A.W., M.K., A.G.S., G.K., and S.C.H.; performed experiments: K.R.M., A.W., M.K., K.T.D., C.E.M., and A.G.S.; analyzed data: K.R.M., A.W., M.K., C.E.M., G.D.S., T.B.K., G.K., and S.C.H.; wrote paper: K.R.M., A.W., M.K., G.K., and S.C.H.; edited paper: K.R.M., A.W., M.K., G.D.S., A.G.S., G.K., and S.C.H.

## DECLARATION OF INTERESTS

The authors declare no competing interests.

Received: June 15, 2017

Revised: October 12, 2017

Accepted: December 8, 2017

Published: January 16, 2018

## REFERENCES

- Adams, P.D., Afonine, P.V., Bunkóczki, G., Chen, V.B., Davis, I.W., Echols, N., Headd, J.J., Hung, L.W., Kapral, G.J., Grosse-Kunstleve, R.W., et al. (2010). PHENIX: a comprehensive Python-based system for macromolecular structure solution. *Acta Crystallogr. D Biol. Crystallogr.* 66, 213–221.
- Andrews, S.F., Huang, Y., Kaur, K., Popova, L.I., Ho, I.Y., Pauli, N.T., Henry Dunand, C.J., Taylor, W.M., Lim, S., Huang, M., et al. (2015). Immune history profoundly affects broadly protective B cell responses to influenza. *Sci. Transl. Med.* 7, 316ra192.
- Brochet, X., Lefranc, M.P., and Giudicelli, V. (2008). IMGT/V-QUEST: the highly customized and integrated system for IG and TR standardized V-J and V-D-J sequence analysis. *Nucleic Acids Res.* 36, W503–8.
- Carsenti, R., Rosado, M.M., and Wardmann, H. (2004). Peripheral development of B cells in mouse and man. *Immunol. Rev.* 197, 179–191.
- CDC (2007). Influenza virus microneutralization assay (Immunology and Pathogenesis Branch/Influenza Division/CDC US Department of Health and Human Services).
- CDC (2009). Influenza Virus Microneutralization Assay H1N1 Pandemic Response (Centers for Disease Control US Department of Health and Human Services).
- Chen, V.B., Arendall, W.B., 3rd, Headd, J.J., Keedy, D.A., Immormino, R.M., Kapral, G.J., Murray, L.W., Richardson, J.S., and Richardson, D.C. (2010). MolProbity: all-atom structure validation for macromolecular crystallography. *Acta Crystallogr. D Biol. Crystallogr.* 66, 12–21.
- Corti, D., Voss, J., Gamblin, S.J., Codoni, G., Macagno, A., Jarrossay, D., Vachieri, S.G., Pinna, D., Minola, A., Vanzetta, F., et al. (2011). A neutralizing antibody selected from plasma cells that binds to group 1 and group 2 influenza A hemagglutinins. *Science* 333, 850–856.
- Dreyfus, C., Laursen, N.S., Kwaks, T., Zuidgeest, D., Khayat, R., Ekiert, D.C., Lee, J.H., Metlagel, Z., Bujny, M.V., Jongeneelen, M., et al. (2012). Highly conserved protective epitopes on influenza B viruses. *Science* 337, 1343–1348.
- Ekiert, D.C., Kashyap, A.K., Steel, J., Rubrum, A., Bhabha, G., Khayat, R., Lee, J.H., Dillon, M.A., O'Neil, R.E., Faynboym, A.M., et al. (2012). Cross-neutralization of influenza A viruses mediated by a single antibody loop. *Nature* 489, 526–532.
- Emsley, P., and Cowtan, K. (2004). Coot: model-building tools for molecular graphics. *Acta Crystallogr. D Biol. Crystallogr.* 60, 2126–2132.
- Fish, S., Zenowich, E., Fleming, M., and Manser, T. (1989). Molecular analysis of original antigenic sin. I. Clonal selection, somatic mutation, and isotype switching during a memory B cell response. *J. Exp. Med.* 170, 1191–1209.
- Fonville, J.M., Wilks, S.H., James, S.L., Fox, A., Ventresca, M., Aban, M., Xue, L., Jones, T.C., Le, N.M.H., Pham, Q.T., et al. (2014). Antibody landscapes after influenza virus infection or vaccination. *Science* 346, 996–1000.
- Haynes, B.F., Kelsoe, G., Harrison, S.C., and Kepler, T.B. (2012). B-cell-lineage immunogen design in vaccine development with HIV-1 as a case study. *Nat. Biotechnol.* 30, 423–433.

- Jackson, K.J., Liu, Y., Roskin, K.M., Glanville, J., Hoh, R.A., Seo, K., Marshall, E.L., Gurley, T.C., Moody, M.A., Haynes, B.F., et al. (2014). Human responses to influenza vaccination show seroconversion signatures and convergent antibody rearrangements. *Cell Host Microbe* 16, 105–114.
- Jensen, K.E., Davenport, F.M., Hennessy, A.V., and Francis, T., Jr. (1956). Characterization of influenza antibodies by serum absorption. *J. Exp. Med.* 104, 199–209.
- Joyce, M.G., Wheatley, A.K., Thomas, P.V., Chuang, G.Y., Soto, C., Bailer, R.T., Druz, A., Georgiev, I.S., Gillespie, R.A., Kanekiyo, M., et al.; NISC Comparative Sequencing Program (2016). Vaccine-Induced Antibodies that Neutralize Group 1 and Group 2 Influenza A Viruses. *Cell* 166, 609–623.
- Kabsch, W. (2010). Xds. *Acta Crystallogr. D Biol. Crystallogr.* 66, 125–132.
- Kallewaard, N.L., Corti, D., Collins, P.J., Neu, U., McAuliffe, J.M., Benjamin, E., Wachter-Rosati, L., Palmer-Hill, F.J., Yuan, A.Q., Walker, P.A., et al. (2016). Structure and Function Analysis of an Antibody Recognizing All Influenza A Subtypes. *Cell* 166, 596–608.
- Kepler, T.B. (2013). Reconstructing a B-cell clonal lineage. I. Statistical inference of unobserved ancestors. *F1000Res.* 2, 103.
- Kilbourne, E.D. (2006). Influenza pandemics of the 20th century. *Emerg. Infect. Dis.* 12, 9–14.
- Kräutler, N.J., Suan, D., Butt, D., Bourne, K., Hermes, J.R., Chan, T.D., Sundling, C., Kaplan, W., Schofield, P., Jackson, J., et al. (2017). Differentiation of germinal center B cells into plasma cells is initiated by high-affinity antigen and completed by Tfh cells. *J. Exp. Med.* 214, 1259–1267.
- Kuraoka, M., Schmidt, A.G., Nojima, T., Feng, F., Watanabe, A., Kitamura, D., Harrison, S.C., Kepler, T.B., and Kelsoe, G. (2016). Complex Antigens Drive Permissive Clonal Selection in Germinal Centers. *Immunity* 44, 542–552.
- Lin, Y.P., Xiong, X., Wharton, S.A., Martin, S.R., Coombs, P.J., Vachieri, S.G., Christodoulou, E., Walker, P.A., Liu, J., Skehel, J.J., et al. (2012). Evolution of the receptor binding properties of the influenza A(H3N2) hemagglutinin. *Proc. Natl. Acad. Sci. USA* 109, 21474–21479.
- Lingwood, D., McTamney, P.M., Yassine, H.M., Whittle, J.R., Guo, X., Boyington, J.C., Wei, C.J., and Nabel, G.J. (2012). Structural and genetic basis for development of broadly neutralizing influenza antibodies. *Nature* 489, 566–570.
- Luo, X.M., Maarschalk, E., O'Connell, R.M., Wang, P., Yang, L., and Baltimore, D. (2009). Engineering human hematopoietic stem/progenitor cells to produce a broadly neutralizing anti-HIV antibody after *in vitro* maturation to human B lymphocytes. *Blood* 113, 1422–1431.
- McCoy, A.J., Grosse-Kunstleve, R.W., Adams, P.D., Winn, M.D., Storoni, L.C., and Read, R.J. (2007). Phaser crystallographic software. *J. Appl. Cryst.* 40, 658–674.
- Moody, M.A., Zhang, R., Walter, E.B., Woods, C.W., Ginsburg, G.S., McClain, M.T., Denny, T.N., Chen, X., Munshaw, S., Marshall, D.J., et al. (2011). H3N2 influenza infection elicits more cross-reactive and less clonally expanded anti-hemagglutinin antibodies than influenza vaccination. *PLoS ONE* 6, e25797.
- Nakamura, G., Chai, N., Park, S., Chiang, N., Lin, Z., Chiu, H., Fong, R., Yan, D., Kim, J., Zhang, J., et al. (2013). An *in vivo* human-plasmablast enrichment technique allows rapid identification of therapeutic influenza A antibodies. *Cell Host Microbe* 14, 93–103.
- Nutt, S.L., Hodgkin, P.D., Tarlinton, D.M., and Corcoran, L.M. (2015). The generation of antibody-secreting plasma cells. *Nat. Rev. Immunol.* 15, 160–171.
- Pappas, L., Foglierini, M., Piccoli, L., Kallewaard, N.L., Turrini, F., Silacci, C., Fernandez-Rodriguez, B., Agatic, G., Giacchetto-Sasselli, I., Pellicciotta, G., et al. (2014). Rapid development of broadly influenza neutralizing antibodies through redundant mutations. *Nature* 516, 418–422.
- Phan, T.G., Paus, D., Chan, T.D., Turner, M.L., Nutt, S.L., Basten, A., and Brink, R. (2006). High affinity germinal center B cells are actively selected into the plasma cell compartment. *J. Exp. Med.* 203, 2419–2424.
- Raymond, D.D., Stewart, S.M., Lee, J., Ferdinand, J., Bajic, G., Do, K.T., Hernandes, M.J., Suphaphiphat, P., Settembre, E.C., Dormitzer, P.R., et al. (2016). Influenza immunization elicits antibodies specific for an egg-adapted vaccine strain. *Nat. Med.* 22, 1465–1469.
- Rogers, G.N., Paulson, J.C., Daniels, R.S., Skehel, J.J., Wilson, I.A., and Wiley, D.C. (1983). Single amino acid substitutions in influenza haemagglutinin change receptor binding specificity. *Nature* 304, 76–78.
- Schmidt, A.G., Xu, H., Khan, A.R., O'Donnell, T., Khurana, S., King, L.R., Manischewitz, J., Golding, H., Suphaphiphat, P., Carfi, A., et al. (2013). Preconfiguration of the antigen-binding site during affinity maturation of a broadly neutralizing influenza virus antibody. *Proc. Natl. Acad. Sci. USA* 110, 264–269.
- Schmidt, A.G., Do, K.T., McCarthy, K.R., Kepler, T.B., Liao, H.X., Moody, M.A., Haynes, B.F., and Harrison, S.C. (2015a). Immunogenic Stimulus for Germline Precursors of Antibodies that Engage the Influenza Hemagglutinin Receptor-Binding Site. *Cell Rep.* 13, 2842–2850.
- Schmidt, A.G., Therkelsen, M.D., Stewart, S., Kepler, T.B., Liao, H.X., Moody, M.A., Haynes, B.F., and Harrison, S.C. (2015b). Viral receptor-binding site antibodies with diverse germline origins. *Cell* 161, 1026–1034.
- Skehel, J.J., and Wiley, D.C. (2000). Receptor binding and membrane fusion in virus entry: the influenza hemagglutinin. *Annu. Rev. Biochem.* 69, 531–569.
- Smith, D.J., Lapedes, A.S., de Jong, J.C., Bestebroer, T.M., Rimmelzwaan, G.F., Osterhaus, A.D., and Fouchier, R.A. (2004). Mapping the antigenic and genetic evolution of influenza virus. *Science* 305, 371–376.
- Su, K.Y., Watanabe, A., Yeh, C.H., Kelsoe, G., and Kuraoka, M. (2016). Efficient Culture of Human Naïve and Memory B Cells for Use as APCs. *J. Immunol.* 197, 4163–4176.
- Tiller, T., Meffre, E., Yurasov, S., Tsuji, M., Nussenzweig, M.C., and Wardemann, H. (2008). Efficient generation of monoclonal antibodies from single human B cells by single cell RT-PCR and expression vector cloning. *J. Immunol. Methods* 329, 112–124.
- Wardemann, H., Yurasov, S., Schaefer, A., Young, J.W., Meffre, E., and Nussenzweig, M.C. (2003). Predominant autoantibody production by early human B cell precursors. *Science* 301, 1374–1377.
- Weisel, F.J., Zuccarino-Catania, G.V., Chikina, M., and Shlomchik, M.J. (2016). A Temporal Switch in the Germinal Center Determines Differential Output of Memory B and Plasma Cells. *Immunity* 44, 116–130.
- Whittle, J.R., Zhang, R., Khurana, S., King, L.R., Manischewitz, J., Golding, H., Dormitzer, P.R., Haynes, B.F., Walter, E.B., Moody, M.A., et al. (2011). Broadly neutralizing human antibody that recognizes the receptor-binding pocket of influenza virus hemagglutinin. *Proc. Natl. Acad. Sci. USA* 108, 14216–14221.
- Whittle, J.R., Wheatley, A.K., Wu, L., Lingwood, D., Kanekiyo, M., Ma, S.S., Narpala, S.R., Yassine, H.M., Frank, G.M., Yewdell, J.W., et al. (2014). Flow cytometry reveals that H5N1 vaccination elicits cross-reactive stem-directed antibodies from multiple Ig heavy-chain lineages. *J. Virol.* 88, 4047–4057.
- WHO (2010). Serological diagnosis of influenza by microneutralization assay (World Health Organization).
- WHO (2011). Manual for the laboratory diagnosis and virological surveillance of influenza (World Health Organization).
- Willis, J.R., Finn, J.A., Briney, B., Sapparapu, G., Singh, V., King, H., LaBranche, C.C., Montefiori, D.C., Meiler, J., and Crowe, J.E., Jr. (2016). Long antibody HCDR3s from HIV-naïve donors presented on a PG9 neutralizing antibody background mediate HIV neutralization. *Proc. Natl. Acad. Sci. USA* 113, 4446–4451.
- Wrammert, J., Koutsonanos, D., Li, G.M., Edupuganti, S., Sui, J., Morrissey, M., McCausland, M., Skountzou, I., Hornig, M., Lipkin, W.I., et al. (2011). Broadly cross-reactive antibodies dominate the human B cell response against 2009 pandemic H1N1 influenza virus infection. *J. Exp. Med.* 208, 181–193.
- Xu, H., Schmidt, A.G., O'Donnell, T., Therkelsen, M.D., Kepler, T.B., Moody, M.A., Haynes, B.F., Liao, H.X., Harrison, S.C., and Shaw, D.E. (2015). Key mutations stabilize antigen-binding conformation during affinity maturation of a broadly neutralizing influenza antibody lineage. *Proteins* 83, 771–780.
- Zhou, T., Georgiev, I., Wu, X., Yang, Z.Y., Dai, K., Finzi, A., Kwon, Y.D., Scheid, J.F., Shi, W., Xu, L., et al. (2010). Structural basis for broad and potent neutralization of HIV-1 by antibody VRC01. *Science* 329, 811–817.

**STAR★METHODS****KEY RESOURCES TABLE**

REAGENT or RESOURCE	SOURCE	IDENTIFIER
<b>Antibodies</b>		
PE/Cy5 Mouse Anti-Human CD3 (UCHT1)	BD Bioscience	CAT#555334
anti-human CD14-Tri (TuK4)	Thermo Scientific	CAT#MHCD1406
PE/Cy5 Mouse Anti-Human CD16 (3G8)	BD Bioscience	CAT#555408
PE/Cy7 anti-human CD19 Antibody (HIB19)	BioLegend	CAT#302216
APC Mouse Anti-Human IgG (G18-145)	BD Bioscience	CAT#550931
APC/Cy7 anti-human IgD Antibody (IA6-2)	BioLegend	CAT#348218
Brilliant Violet 421 anti-human CD27 Antibody (M-T271)	BioLegend	CAT#356418
Brilliant Violet 510 anti-human CD24 Antibody (ML5)	BioLegend	CAT#311126
FITC anti-human IgM Antibody (MHM-88)	BioLegend	CAT#314506
Mouse IgG1 Kappa isotype control (MG1K)	Rockland	CAT#010-001-330
Ferret hyperimmune sera to A/California/07/2009 (H1N1)	BEI Resources	CAT#NR-19261
Ferret hyperimmune sera to A/Solomon Islands/3/2006 (H1N1)	NIH Biodefense and Emerging Infections Research Repository, NIH,NIAID	CAT#NR-19262
Ferret hyperimmune sera to A/USSR/90/1977 (H1N1)	NIH Biodefense and Emerging Infections Research Repository, NIH,NIAID	CAT#FR-953
Ferret hyperimmune sera to A/Fujian/411/2002 (H3N2)	NIH Biodefense and Emerging Infections Research Repository, NIH,NIAID	CAT#FR-1264
Ferret hyperimmune sera to A/Texas/50/2012 (H3N2)	NIH Biodefense and Emerging Infections Research Repository, NIH,NIAID	CAT#FR-1263
Mouse anti-influenza A nucleoprotein clones A1 and A3	BEI Resources	CAT#NR-4282
PE-conjugated Goat anti-human IgG	Southern Biotech	CAT#2040-09
Goat anti-human Kappa-UNLB	Southern Biotech	CAT#2060-01
Goat anti-human Lambda-UNLB	Southern Biotech	CAT#2070-01
Goat anti-human IgG	Jackson ImmunoResearch	CAT#109-005-098
PE conjugated goat anti-mouse IgG	Southern Biotech	CAT#1030-09
<b>Bacterial and Virus Strains</b>		
A/Chile/1/1983 X83 (H1N1)	BEI Resources	CAT#NR-3585
A/Solomon Islands/3/2006 (H1N1)	NIH Biodefense and Emerging Infections Research Repository, NIH,NIAID	CAT#FR-331
A/California/07/2009 (H1N1)	BEI Resources	CAT#NR-19261
A/Shanghai/11/1987 (H3N2)	BEI Resources	CAT#NR-3505
A/Johannesburg/33/1994 (H3N2)	BEI Resources	CAT#NR-3580
A/Wisconsin/67/2005 (H3N2)	NIH Biodefense and Emerging Infections Research Repository, NIH,NIAID	CAT#FR-397
A/Texas/50/2012 (H3N2)	NIH Biodefense and Emerging Infections Research Repository, NIH,NIAID	CAT#FR-1263

(Continued on next page)

***Continued***

REAGENT or RESOURCE	SOURCE	IDENTIFIER
<b>Biological Samples</b>		
Healthy adult-Peripheral blood mononuclear cells		KEL01
Healthy adult-Peripheral blood mononuclear cells		KEL03
Healthy adult-Peripheral blood mononuclear cells		KEL06
<b>Chemicals, Peptides, and Recombinant Proteins</b>		
Human recombinant IL-2	Peprotech	CAT#200-02
Human recombinant IL-4	Peprotech	CAT#200-04
Human recombinant IL-21	Peprotech	CAT#200-21
Human recombinant BAFF	Peprotech	CAT#310-13
HyClone FBS	ThermoFisher	CAT#SH30070.03
7-AAD (7-Aminoactinomycin D)	BD Bioscience	CAT#559925
BD Calibrite Beads	BD Bioscience	CAT#349502
Pierce HRV 3C Protease	ThermoFisher	CAT#88946
TALON® Metal Affinity Resin	Clontech	CAT#635652
Ni Sepharose® Excel	GE Healthcare	CAT#17-3712-02
Perce Protein G Agarose	ThermoFisher	CAT# 20399
Microplex Microspheres regions 1 – 100 (Luminex carboxylated beads)	Luminex Corp	CAT#LC10001-01 – LC10100-01
Lipofectamine® 2000 Transfection Reagent	ThermoFisher	CAT#11668500
Polyethylenimine, Linear, MW 25000, Transfection Grade	Poly Sciences	CAT# 23966-1
<b>Critical Commercial Assays</b>		
Phycoerythrin Labeling Kit-NH2	Dojindo	CAT# LK23-10
Dip and Read Ni-NTA (NTA) Biosensors	ForteBio	CAT# 18-5103
<b>Deposited Data</b>		
Nucleotide sequence. K03.12 lineage	GenBank	KY778717-KY778740
Atomic coordinates, K03.12 UCA HA complex	Protein Data Bank	5W0D
Atomic coordinates, K03.12 HA complex	Protein Data Bank	5W08
<b>Experimental Models: Cell Lines</b>		
MS40L-low	David Baltimore ( <a href="#">Luo et al., 2009</a> ) Garnett Kelsoe ( <a href="#">Su et al., 2016</a> ) This study	N.A
293T	ATCC	CRL-11268
GIBCO® 293-F	ThermoFisher	CAT# 11625019
High Five	ThermoFisher	CAT#B85502
Madin-Darby canine kidney (MDCK)	ATCC	CCL-34
Madin-Darby canine kidney (MDCK)	NIH Biodefense and Emerging Infections Research Repository, NIH,NIAID	FR-58
<b>Recombinant DNA</b>		
pVRC_K03.12_HC_His_Fab	This study	N.A
pVRC_K03.12_HC_3C_His_Fab	This study	N.A
pVRC_K03.12_HC_IgG	This study	N.A
pVRC_K03.12_LC	This study	N.A
pVRC_K03.12_UCA_HC_His_Fab	This study	N.A

(Continued on next page)

***Continued***

REAGENT or RESOURCE	SOURCE	IDENTIFIER
pVRC_K03.12_UCA_HC_IgG	This study	N.A
pVRC_K03.12_UCA_LC	This study	N.A
pVRC_K03.12_I11_HC_3C_His_Fab	This study	N.A
pVRC_K03.12_I11_LC	This study	N.A
pVRC_K03.12_I10_HC_3C_His_Fab	This study	N.A
pVRC_K03.12_I10_LC	This study	N.A
pVRC_K03.12_I4_HC_3C_His_Fab	This study	N.A
pVRC_K03.12_I4_LC	This study	N.A
pVRC_K03.1_HC_3C_His_Fab	This study	N.A
pVRC_K03.1_LC	This study	N.A
pVRC_C05_HC_3C_His_Fab	This study- <a href="#">Ekiert et al., 2012</a>	N.A
pVRC_C05_LC	This study- <a href="#">Ekiert et al., 2012</a>	N.A
pVRC_H2227_HC_3C_His_Fab	This study- <a href="#">Moody et al., 2011</a>	N.A
pVRC_H2227_LC	This study- <a href="#">Moody et al., 2011</a>	N.A
pVRC_H2214_HC_3C_His_Fab	This study- <a href="#">Moody et al., 2011</a>	N.A
pVRC_H2214_UCA_LC	This study- <a href="#">Moody et al., 2011</a>	N.A
pVRC_H2210_HC_IgG	This study- <a href="#">Moody et al., 2011</a>	N.A
pVRC_H2210_UCA_LC	This study- <a href="#">Moody et al., 2011</a>	N.A
pVRC_CH67_HC_IgG (musinized)	Moody et al., <a href="#">2011-Kuraoka et al., 2016</a>	N.A
pVRC_CH67_LC (musinized)	Moody et al., <a href="#">2011-Kuraoka et al., 2016</a>	N.A
pFB_H1_USSR_77_head	<a href="#">Schmidt et al., 2015a</a>	N.A
pFB_H1_Brazil_78_head	<a href="#">Schmidt et al., 2015a</a>	N.A
pFB_H1_Chile_83_head	<a href="#">Schmidt et al., 2015a</a>	N.A
pFB_H1_Kawasaki_86_head	<a href="#">Schmidt et al., 2015a</a>	N.A
pFB_H1_Massachusetts_90_head	<a href="#">Schmidt et al., 2015a</a>	N.A
pFB_H1_Massachusetts_90_FLsE	This Study	N.A
pFB_H1_Massachusetts_90_head_ΔK133a	<a href="#">Schmidt et al., 2015a</a>	N.A
pFB_H1_Bayern_95_head	<a href="#">Schmidt et al., 2015a</a>	N.A
pFB_H1_Beijing_95_head	<a href="#">Schmidt et al., 2015a</a>	N.A
pFB_H1_Florida_00_head	<a href="#">Schmidt et al., 2015a</a>	N.A
pFB_H1_North_Carolina_03_head	<a href="#">Schmidt et al., 2015a</a>	N.A
pFB_H1_Solomon_Islands_06_head	<a href="#">Schmidt et al., 2015a</a>	N.A
pFB_H1_Solomon_Islands_06_head_+K133a	<a href="#">Schmidt et al., 2015a</a>	N.A
pFB_H1_Solomon_Islands_06_FLsE	<a href="#">Whittle et al., 2011</a>	
pFB_H1_California_09_head	<a href="#">Schmidt et al., 2015a</a>	N.A
pFB_H1_California_09_FLsE	This Study	N.A
pFB_H3_Victoria_75_head	This Study	N.A
pFB_H3_X31_FLsE	This Study	N.A
pFB_H3_Bangkok_79_head	This Study	N.A
pFB_H3_Philippines_82_head	This Study	N.A
pFB_H3_Leningrad_86_head	This Study	N.A
pFB_H3_Beijing_89_head	This Study	N.A
pFB_H3_Johannesburg_94_head	This Study	N.A
pFB_H3_Johannesburg_94_trimeric_head	This Study	N.A
pFB_H3_Moscow_99_head	This Study	N.A
pFB_H3_Fujian_02_head	This Study	N.A
pFB_H3_Wisconsin_05_head	This Study	N.A

(Continued on next page)

**Continued**

REAGENT or RESOURCE	SOURCE	IDENTIFIER
pFB_H3_Wisconsin_05_trimeric_head	This Study	N.A
pFB_H3_Wisconsin_05_FLsE	This Study	N.A
pFB_H3_Brisbane_07_head	This Study	N.A
pFB_H3_Perth_09_head	This Study	N.A
pFB_H3_Victoria_11_head	This Study	N.A
pFB_H3_Texas_12_head	This Study	N.A
pFB_H3_South_Australia_2014_head	This Study	N.A
pFB_H5_Vietnam_04_FLsE	This Study	N.A
pFB_B_Malaysia_FLsE	This Study	N.A
Software and Algorithms		
FlowJo	Treestar Inc	<a href="https://www.flowjo.com/">https://www.flowjo.com/</a>
FACSDIVA	BD Biosciences	<a href="http://www.bd-biosciences.com/us/instruments/research/software/flow-cytometry-acquisition/bd-facsdiva-software/m/111112/overview">http://www.bd-biosciences.com/us/instruments/research/software/flow-cytometry-acquisition/bd-facsdiva-software/m/111112/overview</a>
XDS	Kabsch, 2010	<a href="http://xds.mpimf-heidelberg.mpg.de/">http://xds.mpimf-heidelberg.mpg.de/</a>
PHASER	McCoy et al., 2007	<a href="http://www.phaser.cimr.cam.ac.uk/index.php/Phaser_Crystallographic_Software">http://www.phaser.cimr.cam.ac.uk/index.php/Phaser_Crystallographic_Software</a>
Coot	Emsley & Cowtan, 2004	
PHENIX	Adams et al., 2010	<a href="http://www2.mrc-lmb.cam.ac.uk/personal/pemsley/coot/">http://www2.mrc-lmb.cam.ac.uk/personal/pemsley/coot/</a>
PyMol	Schrödinger, LLC	<a href="http://www.pymol.org">http://www.pymol.org</a>
MolProbity	Chen et al., 2010	<a href="http://molprobity.biochem.duke.edu">http://molprobity.biochem.duke.edu</a>
BLItz Pro Software	ForteBio	<a href="https://www.blitzmenow.com/blitz_pro.html">https://www.blitzmenow.com/blitz_pro.html</a>
Clonalyst	Kepler, 2013	<a href="http://www.bu.edu/computationalimmunology/research/software/">http://www.bu.edu/computationalimmunology/research/software/</a>
IMGT/V-QUEST	Brochet et al., 2008	<a href="http://www.imgt.org/IMGT_vquest/vquest">http://www.imgt.org/IMGT_vquest/vquest</a>
Other		
Pathogen Free embryonated chicken eggs	Sunrise Farms or Charles River Avian Vaccine Services	CAT#10100326

**CONTACT FOR REAGENT AND RESOURCE SHARING**

Further information and requests for resources and reagents should be directed to the lead contact, Stephen C. Harrison ([harrison@crystal.harvard.edu](mailto:harrison@crystal.harvard.edu)).

**EXPERIMENTAL MODEL AND SUBJECT DETAILS****Subject Details**

Peripheral blood mononuclear cells (PBMCs) were obtained from three human (*Homo sapiens sapiens*) subjects under Duke Institutional Review Board committee guidelines. Written informed consent was obtained from all three subjects. Human subjects are designated KEL01 (male, adult, age 39), KEL03 (female, adult, age 39) and KEL06 (female, adult, age 35).

**Cell Lines**

Human embryonic kidney (HEK) 293T cells were maintained at 37° degrees Celsius with 5% CO<sub>2</sub> in DMEM supplemented with 10% FBS, penicillin and streptomycin. Human 293F cells were maintained at 37° degrees Celsius with 5% CO<sub>2</sub> in FreeStyle 293 Expression Medium (ThermoFisher) supplemented with penicillin and streptomycin. MS40L-low feeder cells (*Mus musculus*) were expanded from frozen aliquots in Iscove's Modified Dulbecco's Medium (Invitrogen) containing 10% HyClone FBS (Thermo scientific), 2-mercaptoethanol (5.5 × 10<sup>-5</sup> M), penicillin (100 units/ml), and streptomycin (100 µg/ml; all Invitrogen) at 37° degrees Celsius with 5% CO<sub>2</sub> ([Luo et al., 2009](#); [Su et al., 2016](#)). Madin-Darby canine kidney cells (MDCK) (*Canis lupus familiaris*) were maintained in DMEM at 37° degrees Celsius with 5% CO<sub>2</sub>. High Five Cells (BTI-TN-5B1-4) (*Trichoplusia ni*) were maintained at 28° degrees Celsius in either EX-CELL 405 medium (Sigma) supplemented with penicillin and streptomycin or Express-Five (Thermo Fisher) medium supplemented with L-glutamine (GIBCO) at a final concentration of 16 mM, penicillin and streptomycin. Cell lines were not subject to authentication.

## Subject-Derived Cells

Human Bmem cells were expanded in the presence of MS40L-low feeder cells as described (Luo et al., 2009; Su et al., 2016), with the following modifications. Single human Bmem cells were directly sorted into each well of 96-well plates and cultured with MS40L-low feeder cells in RPMI1640 (Invitrogen) containing 10% HyClone FBS (Thermo scientific), 2-mercaptoethanol ( $5.5 \times 10^{-5}$  M), penicillin (100 units/ml), streptomycin (100 µg/ml), HEPES (10 mM), sodium pyruvate (1 mM), and MEM nonessential amino acid (1 × ; all Invitrogen). Exogenous recombinant human IL-2 (50 ng/ml), IL-4 (10 ng/ml), IL-21 (10 ng/ml) and BAFF (10 ng/ml; all Peprotech) were added to cultures. Cultures were maintained at 37° degrees Celsius with 5% CO<sub>2</sub>. Half of the culture medium was replaced twice weekly with fresh medium (with fresh cytokines).

## METHOD DETAILS

### Clinical Samples

KEL01 and KEL03 received the trivalent inactivated seasonal influenza vaccine (TIV) 2014-2015 Fluvirin, which contained A/Christchurch/16/2010, NIB-74 (H1N1), A/Texas/50/2012, NYMC X-223 (H3N2), and B/Massachusetts/2/2012, NYMC BX-51B. KEL06 received the TIV 2015-2016 Flucelvax, which contained A/Brisbane/10/2010 (H1N1), A/South Australia/55/2014 (H3N2), and B/Utah/9/2014. Blood was drawn on day 14 post-vaccination and PBMCs isolated by centrifugation over Ficoll density gradients (SepMate-50 tubes, StemCell Tech). Cell samples were frozen and kept in liquid nitrogen until use.

### Flow Cytometry and Human Bmem Cell Definition

Human Bmem cells were isolated by flow cytometry. PBMCs in RPMI containing 10% FBS were incubated with excess mouse IgG1 (MG1K; Rockland), to block nonspecific binding, and then labeled with fluorochrome-conjugated mAbs. The following human surface antigen specific mAbs were used: anti-human IgM-FITC (MHM-88), CD3-PE-Cy5 (UCHT1), CD14-Tri (TuK4), CD16-PE-Cy5 (3G8), CD19-PE-Cy7 (HIB19), IgG-APC (G18-145), IgD-APC-Cy7 (IA6-2), CD27-BV421 (M-T271), and CD24-BV510 (ML5), purchased from BD Biosciences or BioLegend or Thermo Scientific. PE-labeled HA A/Wisconsin/67/2005 (H3N2) was prepared using R-Phycoerythrin Labeling Kit-NH2 (Dojindo). Labeled cells were sorted by FACS Vantage with Diva software (BD Biosciences). Flow cytometric data were analyzed with FlowJo software (Treestar Inc.). Doublets were excluded from cell sorting by combinations of FSC-A versus FSC-H gating. Cells positive for 7-AAD (BD Bioscience) or positive for CD3, CD14, or CD16 expression were also excluded. BD Calibrite Beads (BD Biosciences) were used to count numbers of B cells in cultures. Single Bmem cells were directly sorted into each well of 96-well plates and co-cultured with the with MS40L-low feeder line cells (Luo et al., 2009; Su et al., 2016).

### Single-Cell Cultures for Human Bmem Cells

On day 25, culture supernatants were harvested for screening the reactivity of clonal IgG Abs. Expanded clonal B cells were frozen for V(D)J sequence analyses.

### BCR Rearrangement Amplification and Analysis

Rearranged V(D)J gene sequences for human Bmem cells from single-cell cultures were obtained as described (Kuraoka et al., 2016) with modification for the amplification of human Ig genes. Total RNA was extracted from frozen cell pellets of individual single-cell cultures, treated with DNase I, and used for cDNA synthesis. Synthesized cDNA was subjected to two rounds of PCR using Herculase II fusion DNA polymerase (Agilent Technologies) with established primers (Tiller et al., 2008; Wardemann et al., 2003). PCR conditions (both primary and secondary PCR) were 94°C for 4 min, followed by 30 (for primary) or 40 cycles (for secondary) at 94°C for 30 s, 58°C (IgH) for 30 s or 68°C (Igκ/Igλ) for 20 s, and 72°C for 30 s. V(D)J amplicands were gel purified, ligated into vectors, and transformed into bacteria (Kuraoka et al., 2016). DNA sequences were obtained at the Duke DNA sequencing facility. V(D)J rearrangements were identified with Cloanalyst (Kepler, 2013) and IMGT/V-QUEST (<http://imgt.cines.fr>) (Brochet et al., 2008). The lineages of twelve IgG and IgL that avidly bound rHAs of both H1 and H3 subtypes were analyzed using the Cloanalyst program (Kepler, 2013).

### Multiplex Bead Assay

Specificity and avidity of clonal IgG Abs in culture supernatants were determined in a multiplex bead Luminex assay (Luminex Corp.). Culture supernatants and a monoclonal standard, Ab2210, which binds HA H3 WI-05 (Moody et al., 2011), were serially diluted in 1 × PBS containing 1% BSA, 0.05% NaN<sub>3</sub> and 0.05% Tween20 (assay buffer) with 1% milk and incubated for 2 h with the mixture of antigen-coupled microsphere beads in 96-well filter bottom plates (Millipore). After washing three times with assay buffer, beads were incubated for 1 h with PE-conjugated goat anti-human IgG Abs (Southern Biotech). After three washes, the beads were re-suspended in assay buffer and the plates read on a Bio-Plex 3D Suspension Array System (Bio-Rad). The following antigens were coupled with carboxylated beads (Luminex Corp): BSA, goat anti-human Igκ, goat anti-human Igλ (both Southern Biotech), goat anti-human IgG (Jackson ImmunoResearch), and a panel of recombinant hemagglutinins (full-length constructs of H1 A/Solomon Islands/03/2006, H1 A/Massachusetts/1/1990, H1 A/California/04/2009, H1 A/reassortant NYMC X-181 (California/07/2009 × NYMC X-157), H3 A/Wisconsin/67/2005, H3 A/Aichi/2/1968 (X31), H5 A/Vietnam/1203/2004, and B/Malaysia/2506/2004; and trimeric, head-only rHA constructs of H3 A/Wisconsin/67/2005, H3 A/Aichi/2/1968

(X31), and H3 A/Johannesburg/33/1994). For each culture supernatant sample, concentrations of total IgG and rHA H3 WI-05-binding IgG were determined with reference to Ab2210 (Moody et al., 2011). The specific activity for Ab2210 was determined as a binding ratio, bound IgG<sub>Ag</sub>/bound IgG<sub>total</sub>, and defined as equal to 1.0. The avidity index, AvIn—the ratio of [bound IgG<sub>Ag</sub>] to [bound IgG<sub>total</sub>] for each sample—therefore represents the antigen-binding capacity of each clonal IgG relative to Ab2210 (Kuraoka et al., 2016).

### CH67 Inhibition Assay

Diluted (1:10) supernatants from cultures of H3/H1 crossreactive Bmem cells or from B cell negative cultures (mock culture) were incubated overnight with Luminex beads coupled with HA H1 SI-06. Beads were then incubated for 2 h with 2 ng/ml of “musinized” CH67 chimeric Ab, which carries variable regions of CH67 with mouse C<sub>H</sub> and C<sub>L</sub> (Kuraoka et al., 2016). After washing plates, beads were incubated for 1 h with PE-conjugated goat anti-mouse IgG Abs (Southern Biotech), and the plates were read on a Bio-Plex 3D Suspension Array System as described above. Threshold MFI values were set at the point representing mean ± 3SD of mock culture samples.

### Recombinant Fab Expression and Purification

Synthetic heavy- and light-chain variable domain genes for inferred lineage-member and for C05, 2227 and 2214 Fabs were cloned into a modified pVRC8400 expression vector, as previously described (Schmidt et al., 2013). Fab fragments used in crystallization were produced with a C-terminal noncleavable 6xhistidine (6xHis) tag. Fab fragments used for binding studies were cloned into a pVRC8400 vector that was further modified by the introduction of a rhinovirus 3C protease cleavage site between the heavy chain constant domain and C-terminal 6xHis tag.

The K03.12 Fab fragment for crystallization was produced by Lipofectamine 2000 (Thermo Fisher) facilitated, transient transfection of 293T cells. Transfections were carried out in Opti-MEM which was exchanged for FreeStyle 293 Expression Medium for expression 4 hours post transfection. All other Fab fragments were produced by polyethylenimine (PEI) facilitated, transient transfection of 293F cells. Transfection complexes were prepared in Opti-MEM and added to cells that had been resuspended in antibiotic-free medium one hour pre-transfection. Supernatants were harvested 4–5 days post transfection and clarified by low-speed centrifugation. Fabs were purified by passage over Co-NTA agarose (Clontech) followed by gel filtration chromatography on Superdex 200 (GE Healthcare) in 10 mM Tris-HCl, 150 mM NaCl at pH 7.5 (buffer A).

For binding studies the 6xHis tag were removed from Fabs by treatment with PreScission protease (MolBioTech; ThermoScientific) and the protein repurified on Co-NTA agarose followed by gel filtration chromatography on Superdex 200 (GE Healthcare) in buffer A to remove the protease, tag, and uncleaved protein.

### Recombinant IgG Expression and Purification

The heavy chain variable domains of UCA and K03.12 were cloned into pVRC8400 modified to express a full length human IgG1 heavy chain. IgGs were produced by transient transfection of 293F cells as specified above. Five days post-transfection supernatants were harvested, clarified by low-speed centrifugation, adjusted to pH 5 by addition of 1M 2-(N-morpholino)ethanesulfonic acid (MES) (pH 5.0), and incubated overnight with Pierce Protein G Agarose resin (Pierce, Thermo Fisher). The resin was collected in a chromatography column, washed with a column volume of 100mM sodium chloride 20mM (MES) (pH 5.0) and eluted in 0.1M Glycine (pH 2.5) which was immediately neutralized by 1M tris(hydroxymethyl)aminomethane (pH 8).

### Recombinant HA Expression and Purification

All recombinant (HA) constructs were expressed by infection of insect cells with recombinant baculovirus as previously described (Raymond et al., 2016; Schmidt et al., 2013; Whittle et al., 2011; Xu et al., 2015). In brief, synthetic DNA corresponding to the full-length ectodomain or globular HA-head were subcloned into a pFastBac vector modified to encode a C-terminal thrombin cleavage site, a T4 fibritin (foldon) trimerization tag, and a 6xHis tag. The resulting baculoviruses produce HA-trimers and trimeric HA-heads. Monomeric HA-heads were produced by subcloning DNAs corresponding to the HA-head domain into a pFastBac vector modified to encode a C-terminal rhinovirus 3C protease site and a 6xHis tag.

Supernatant from recombinant baculovirus infected High Five Cells (*Trichoplusia ni*) was harvested 72 h post infection and clarified by centrifugation. For HA-trimmers, trimeric HA-heads and the A/Texas/50/2012 (H3N2) HA-head used for crystallization, High Five Cells were maintained in EX-CELL 405 medium (Sigma) supplemented with penicillin and streptomycin. Proteins were purified by adsorption to cobalt-nitrilotriacetic acid (Co-NTA) agarose resin (Clontech), followed by a wash in buffer A, a second wash (trimers only) with buffer A plus 5 mM imidazole, elution in buffer A plus 350mM imidazole (pH 8) and gel filtration chromatography on a Superdex 200 column (GE Healthcare) in buffer A. For expression of all other HA- HA-heads, High Five Cells were maintained in Express-Five (Thermo Fisher) medium supplemented with L-glutamine (GIBCO) to a final concentration of 16 mM, penicillin and streptomycin. Clarified supernatants were passed over Ni-Sepharose excel (GE Healthcare Life Science), followed by the same wash and elution steps as above. The eluted sample was dialyzed overnight against phosphate-buffered saline (PBS) (pH 7.2) using Spectra/Por dialysis membranes (Spectrum Laboratories inc.) with a 6–8 kD molecular weight cutoff. Protein was purified by elution from Co-NTA and gel filtration chromatography, as described above.

### Biolayer Interferometry (BLI)

Binding of Fabs with HA heads was analyzed by BLI (BLItz: forteBIO; Pall); all measurements were in buffer A at room temperature. Purified HA-head was immobilized on a Ni-NTA biosensor, and Fabs (with tag removed by PreScission protease cleavage) were titrated to obtain rate constants and affinities.

### Virus Propagation

Influenza virus strains A/Shanghai/11/1987 X-99a (H3N2), A/Johannesburg/33/1994 X-123a (H3N2) and A/Texas/50/2012 (H3N2) were propagated in Madin-Darby canine kidney (MDCK; ATCC CCL-34) cells, and strains A/Chile/1/1983 X-83 (H1N1), A/Wisconsin/67/2005 (H3N2), A/Solomon Islands/3/2006 (H1N1), and A/California/07/2009 (H1N1)pdm09, in embryonated, specific-pathogen-free, chicken-hen eggs (Sunrise Farms Inc., Catskill, NY or Charles River Avian Vaccine Services, Norwich, CT). Stocks were harvested as pooled and clarified cell culture supernatant/lysate or egg allantoic/amniotic fluid respectively and stored at -80°C. Stocks were titered by tissue culture infectious dose 50 percent (TCID<sub>50</sub>) assay as described for standard procedures ([CDC, 2007, 2009](#); [WHO, 2010, 2011](#)).

### Influenza Microneutralization Assay

Virus neutralization endpoint titers (EPT) were determined using the influenza microneutralization (MN) assay as described ([CDC, 2007, 2009](#); [WHO, 2010, 2011](#)). Briefly, monoclonal antibodies were diluted to test concentration in assay diluent and evaluated as duplicate two fold dilutions series. Absorbance was measured using a Synergy H1 microplate reader (BioTek Instruments Inc., Winooski, Vermont).

### Crystallization

Fab fragments of K03.12 and UCA were incubated at a 1.2:1 molar ratio with the HA-head domain of A/Texas/50/2012 (H3N2) and A/Solomon Islands/3/2006 (H1N1), respectively. Stoichiometric 1:1 complexes were purified by gel filtration chromatography on Superdex 200 in buffer A. The complexes were concentrated to 14-15mg/ml. Crystals of K03.12- A/Texas/50/2012 (H3N2)-head complex were grown in hanging drops over a reservoir of 100 mM sodium citrate/ citric acid (pH 5.5) and 20% (w/v) poly(ethylene glycol) 3000. Crystals were cryoprotected in 180 mM sodium chloride, 120mM sodium citrate/ citric acid (pH 5.6), 24% (w/v) polyethylene glycol 3000 and 20% (v/v) glycerol, added directly to the drop, harvested, and flash cooled in liquid nitrogen. Crystals of complexed UCA-A/Solomon Islands/3/2006 (H1N1)-HA-head were grown in hanging drops over a reservoir of 200mM sodium chloride, 100mM piperazine-N,N'-bis(2-ethanesulfonic acid) (PIPES) (pH 6.0) and 20% (w/v) poly(ethylene glycol) methyl ether 2000. Crystals were cryoprotected in 420mM sodium chloride, 120mM 2-(N-morpholino)ethanesulfonic acid (MES), pH 6.0, 24% (w/v) poly(ethylene glycol) methyl ether 2000 and 14% (v/v) glycerol, added directly to the drop, harvested, and flash cooled in liquid nitrogen.

### Structure Determination and Refinement

We recorded diffraction data at beamlines 8.2.2 at the Advanced Light Source and 24-ID-C at the Advanced Photon Source for complexes of K03.12-A/Texas/50/2012 (H3N2)-head complex and UCA-A/Solomon Islands/3/2006 (H1N1)-HA-head complex, respectively. For the former, four datasets from a single cluster of crystals were processed and merged with XDS ([Kabsch, 2010](#)). Molecular replacement (MR) was carried out with PHASER ([McCoy et al., 2007](#)), using four search models: the HA-head domain from PDB: 4O5N, C<sub>H</sub>C<sub>L</sub> from PDB: 4WUK, V<sub>H</sub> from PDB: 4HKX and from V<sub>L</sub> PDB: 3TNN. There were six copies in the asymmetric unit (ASU). Refinement was performed with PHENIX ([Adams et al., 2010](#)) and model modifications, with COOT ([Emsley and Cowtan, 2004](#)). Refinement of atomic positions and B factors was followed by translation-liberation-screw (TLS) parameterization and placement of water molecules. Six-fold non-crystallographic symmetry (NCS) restraints were imposed throughout refinement. Data from a single crystal of UCA-A/Solomon Islands/3/2006(H1N1)-HA-head were processed with XDS. The search model for UCA-A/Solomon Islands/3/2006 (H1N1)-HA-head was separated into three components; the HA-head domain from PDB: 5UGY, the V<sub>H</sub>V<sub>L</sub> from the K03.12-A/Texas/50/2012 (H3N2)-head complex, and C<sub>H</sub>C<sub>L</sub> from antibody CH65 (PDB: 4WUK). There was one copy in the asymmetric unit. We refined atomic positions and B factors, followed by translation-liberation-screw (TLS) parameterization and placement of water molecules, all in PHENIX ([Adams et al., 2010](#)) and validated final coordinates with the MolProbity server ([Chen et al., 2010](#)). The data collection and refinement statistics are in Table S3. Figures were made with PyMOL (Schrödinger, New York, NY).

## QUANTIFICATION AND STATISTICAL ANALYSIS

### Binding Studies

K<sub>D</sub> values were obtained by applying a 1:1 binding isotherm using vendor-supplied software ("Advanced Kinetics" program). For screening, binding was tested with Fab at 30 μM to determine an apparent K<sub>D</sub>. For selected Fab-HA pairs, Fab was then titrated at a minimum of four different concentrations (chosen depending on the apparent K<sub>D</sub> from the 30 μM concentration) and K<sub>D</sub> obtained by a global fit of the titration curves. Number of curves fit for A/Florida/904/2000 (H1N1): UCA n = 5, I-11 n = 5, I10 n = 4, K03.12 n = 5, I-4 n = 6, and K03.1 n = 5. Number of curves fit for A/Texas/50/2012 (H3N2): UCA n = 4, I-11 n = 4, I10 n = 6, K03.12 n = 7, I-4 n = 5, and K03.1 n = 5. Standard error of the mean is reported in [Figure 4](#) for measurements of k<sub>on</sub> and k<sub>off</sub>.

**Neutralization Assays**

Monoclonal antibodies were diluted to test concentration in assay diluent and evaluated as duplicate two-fold dilutions series. The 50% neutralization EPT for a given sample is reported as the geometric mean of duplicate dilution series.

**DATA AND SOFTWARE AVAILABILITY**

V(D)J sequences for the 12 members of K03.12 lineage are available at GenBank ([www.ncbi.nlm.nih.gov/Genbank](http://www.ncbi.nlm.nih.gov/Genbank)), accession numbers KY778717-KY778740. Coordinates and diffraction data have been deposited at the PDB, accession numbers 5W08 and 5W0D.